

The Anglo-Australian Observatory 2dF facility

I. J. Lewis,^{1,2*} R. D. Cannon,¹ K. Taylor,^{1,3} K. Glazebrook,^{1,4} J. A. Bailey,¹ I. K. Baldry,^{1,4} J. R. Barton,¹ T. J. Bridges,¹ G. B. Dalton,² T. J. Farrell,¹ P. M. Gray,^{1,5} A. Lankshear,¹ C. McCowage,¹ I. R. Parry,^{1,6} R. M. Sharples,⁷ K. Shortridge,¹ G. A. Smith,¹ J. Stevenson,¹ J. O. Straede,¹ L. G. Waller,¹ J. D. Whittard,¹ J. K. Wilcox¹ and K. C. Willis^{1,8}

¹Anglo-Australian Observatory, PO Box 296, Epping, NSW 1710, Australia

²Department of Physics, Keble Road, Oxford OX1 3RH

³Department of Astronomy, California Institute of Technology, Pasadena, CA 91125-2400, USA

⁴Department of Physics and Astronomy, Johns Hopkins University, 3400 North Charles Street, Baltimore, MD 21218-2686, USA

⁵ESO Paranal Observatory, PO Box 540, Antofagasta, Chile

⁶Institute of Astronomy, Madingley Road, Cambridge CB3 0HA

⁷Department of Physics, University of Durham, South Road, Durham DH1 3LE

⁸Australian Centre for Field Robotics, Rose Street, Building J04, University of Sydney, NSW 2006, Australia

Accepted 2002 January 11. Received 2001 December 18; in original form 2001 August 8

ABSTRACT

The 2dF (Two-degree Field) facility at the prime focus of the Anglo-Australian Telescope provides multiple-object spectroscopy over a 2° field of view. Up to 400 target fibres can be independently positioned by a complex robot. Two spectrographs provide spectra with resolutions of between 500 and 2000, over wavelength ranges of 440 and 110 nm respectively. The 2dF facility began routine observations in 1997.

2dF was designed primarily for galaxy redshift surveys and has a number of innovative features. The large corrector lens incorporates an atmospheric dispersion compensator, essential for wide wavelength coverage with small-diameter fibres. The instrument has two full sets of fibres on separate field plates, so that re-configuring can be done in parallel with observing. The robot positioner places one fibre every 6 s, to a precision of 0.3 arcsec (20 μm) over the full field. All components of 2dF, including the spectrographs, are mounted on a 5-m diameter telescope top end ring for ease of handling and to keep the optical fibres short in order to maximize UV throughput.

There is a pipeline data reduction system which allows each data set to be fully analysed while the next field is being observed.

2dF has achieved its initial astronomical goals. The redshift surveys obtain spectra at the rate of 2500 galaxies per night, yielding a total of about 200 000 objects in the first four years. Typically a $B = 19$ galaxy gives a spectrum with a signal-to-noise ratio of better than 10 per pixel in less than an hour; redshifts are derived for about 95 per cent of all galaxies, with 99 per cent reliability or better. Total system throughput is about 5 per cent. The failure rate of the positioner and fibre system is about 1:10 000 moves or once every few nights, and recovery time is usually short.

In this paper we provide the historical background to the 2dF facility, the design philosophy, a full technical description and a summary of the performance of the instrument. We also briefly review its scientific applications and possible future developments.

Key words: instrumentation: spectrographs – techniques: spectroscopic – surveys – galaxies: distances and redshifts – large-scale structure of Universe.

*E-mail: ijl@astro.ox.ac.uk

1 INTRODUCTION

The value of equipping telescopes with a large field of view has been recognized for some time. In 1986 the Royal Astronomical Society report ‘Review of Scientific Priorities for UK Astronomical Research 1990–2000’ (Royal Astronomical Society 1986) put a wide-field multi-object spectroscopic facility at the top of its priority list for new projects. Subsequently the UK Large Telescope Panel recommended that a wide-field survey facility be pursued in tandem with an 8-m-telescope project.

The general scientific case for a wide-field spectroscopic facility on a 4-m telescope was twofold: to provide spectra for large samples of objects found in the multi-colour imaging surveys from the UK, European Southern Observatory (ESO) and Oschin (Palomar) Schmidt telescopes; and to generate targets for the coming generation of 8–10 m optical telescopes. The biggest specific science driver was to obtain redshifts of tens or even hundreds of thousands of galaxies and quasars, to elucidate the three-dimensional structure and evolution of the Universe. Other major projects required spectra for large samples of stars, to determine their kinematics and composition and hence the dynamical and chemical history of our Galaxy; for similar studies of the Magellanic Clouds; and for detailed studies of star clusters and clusters of galaxies.

One possibility was to provide a multi-fibre upgrade to the 3.9-m Anglo-Australian Telescope (AAT). This was particularly advantageous for two reasons. First, the optical design of the telescope (a hyperboloidal primary mirror and relatively slow f -ratio of $f/3.3$ at prime focus) enabled a wide field of 2° to be achieved using a large but straightforward optical corrector. Secondly, the Anglo-Australian Observatory (AAO) already had extensive experience with multi-object fibre spectroscopy. This dates from the pioneering days of optical fibres and its brass plug-plate system FOCAP (Gray 1983) and more recently the fully automated AUTOFIB fibre positioner system (Parry & Gray 1986).

At the end of 1988 the AAT Board (AATB) commissioned a full design study of a wide-field fibre optic spectroscopic facility for the AAT (Taylor & Gray 1990). Following further detailed investigations into cost and budgets, and in the expectation of some additional funding from both the Australian and UK Governments, the AATB gave its approval to begin the Two-degree Field (or 2dF) project in 1990 March. Initially the direct budget allocated was A\$2.25 million (for components and certain specific tasks which could not be done in-house) and it was expected to take 4–5 years to complete. Since the project would dominate the activities of the AAO for several years, a Project Management Committee was established with several external expert members.

In developing the 2dF facility the AAO wished to build on the techniques already used for the fully automated AUTOFIB instrument in use at the Cassegrain focus of the AAT. Since 2dF would offer almost an order of magnitude increase in multiplex advantage over AUTOFIB and would be located at the more challenging prime focus, several technical problems had to be solved before final approval was given for commencement of the project.

The technical problems were addressed in the initial design study reports and covered areas such as the accuracy required of the robotic positioner, the design of the fibre retraction systems, the location and design of the fibre spectrographs and the requirement for a double fieldplate system to maximize observing time.

The mechanical constraints were eased by the strength and

rigidity of the telescope tube structure and the size of the dome, which meant that a large instrument could be housed at prime focus without clearance and flexure problems.

Commissioning of the 2dF facility began with the new prime-focus corrector in the latter part of 1993. The instrument was officially declared open at a ceremony on 1995 November 20, and the first spectroscopic data were obtained in mid-1996. The facility began to provide scheduled scientific observations in 1997 September with almost full functionality. The project ran about 40 per cent over the original time estimate and 20 per cent over budget (these two are linked, in that 2dF could have been completed sooner had more funds been available). The effective total cost was subsequently estimated to have been about A\$8 million, including all staff costs and overheads. The bulk of the design and construction work was eventually done in-house using the AAO facilities in Sydney and Coonabarabran, partly because many aspects involved innovative design features which could not be easily specified or contracted out, and partly to contain costs.

Progress reports describing the evolution of the design of 2dF have been published (Gray & Taylor 1990; Gray et al. 1993; Taylor, Cannon & Watson 1996b; Cannon 1997; Lewis, Glazebrook & Taylor 1998a,b) and project updates have featured regularly in the quarterly AAO Newsletter.

In this paper we provide a full technical description of the 2dF facility and its performance. Section 2 gives an overview of the instrumentation and its relationship to other multiple-object fibre spectroscopy systems. In Section 3, a detailed description of the individual components of the 2dF facility is given. Operation of the 2dF facility is covered in Section 4 and actual performance is detailed in Section 5. Sections 6 and 7 describe the range of projects being done with 2dF and some scientific possibilities for the future. Up-to-date technical information and signal-to-noise ratio calculators are available on the 2dF WWW pages (<http://www.aao.gov.au/2df/>).

2 OVERVIEW OF INSTRUMENT

2.1 Objectives and design philosophy

The 2dF facility was developed with the aim of providing the AAT with a dedicated prime-focus spectroscopy facility, with order of magnitude improvements over existing systems in terms of the field area and number of objects that it is possible to observe simultaneously (the multiplex advantage). While 2dF was designed from the outset to be a versatile common-user instrument, suitable for a wide range of astronomical projects on an international research facility, it was always clear that the dominant project would be to obtain redshifts and hence distances for a very large sample of galaxies (a few times 10^5 objects), to map out the three-dimensional structure of the relatively local Universe.

Two separate but linked large redshift surveys were the initial main projects with 2dF: one for 250 000 galaxies brighter than $b_J = 19.45$ with a median redshift of 0.1 (Colless et al. 2001) and one for 30 000 colour-selected quasars covering redshifts up to 4 (Croom et al. 2001). This meant that 2dF had to be optimized to obtain low-dispersion spectra of a few thousand targets per night, over a wide wavelength range, for mainly non-stellar objects which were in the magnitude range $15 < B < 20$ and spread across more than 1000 square degrees of sky. These requirements are very well met by a system providing two sets of 400 fibres covering 3 square degrees of sky, and capable of reconfiguring one set of fibres in

about an hour, which happens to be equal to the time needed to take adequate signal-to-noise ratio spectra of 19–20 mag galaxies.

Whenever choices had to be made on design features, instrument parameters or priorities, the driver was to maximize the efficiency of 2dF as a redshift engine. The requirements of other projects, such as taking higher resolution spectra of stars, doing longer integrations on fainter galaxies, or working on densely clustered targets, were incorporated where possible, but not if they involved any compromise of performance for the redshift surveys.

2.2 Other multi-fibre systems

Previous multi-object fibre spectroscopy systems on 4-m-class telescopes have used smaller fields of view and significantly smaller multiplex advantage. For example, the William Herschel Telescope AUTOFIB-2 (Parry et al. 1994) and WYFOS (Jenkins et al. 1993) instruments provide fibre spectroscopy of up to 150 objects over a 1° field (40 arcmin unvignetted). The HYDRA instrument (Barden et al. 1994) on the 3.5-m WIYN telescope uses approximately 100 optical fibres to cover an unvignetted field of 1° . Earlier fibre instruments on the AAT were FOCAP with 50 fibres (Gray 1983) and AUTOFIB with 64 fibres (Parry & Gray 1986), both covering a 40-arcmin field at the Cassegrain focus.

Some smaller telescopes offer a larger field of view or larger multiplex advantage. For example, the 2.5-m DuPont telescope at Las Campanas with a 2.1° field and up to 200 optical fibres (Shectman 1993) has been used for the largest previous galaxy redshift survey. At the 1.2-m UK Schmidt Telescope the FLAIR fibre system with 92 fibres covered a 6° field (Watson et al. 1993). FLAIR has now been replaced by a semi-automatic successor: 6dF (Parker, Watson & Miziarski 1998) with 150 fibres. The 2.5-m Sloan Digital Sky Survey (SDSS) telescope has a 3° field of view and 640 optical fibres; this is a dedicated telescope carrying out both multi-colour imaging and a spectroscopic survey of a million galaxies (York et al. 2000). Multi-object systems are also being built for several of the new 8–10 m class telescopes; these will be able to observe fainter objects but cover much smaller fields of view.

2.3 Key features of 2dF

Multi-object fibre systems come in three varieties: plug plates or other off-line field preparation, for example the SDSS fibre system; ‘fishermen around the pond’ type instruments with separate remotely controlled mechanisms to place each fibre simultaneously at a target position, for example MX (Hill & Lesser 1986) and MEFOS (Guerin et al. 1993); and ‘pick and place’ systems involving consecutive placement of fibres with a single complex robot. The most versatile are the single-robot systems, but they have the drawback that placing the fibres consumes a significant amount of observing time. 2dF gets around this drawback by having two independent sets of 400 fibres and two field plates, mounted back-to-back on a tumbler assembly within the instrument. While one set of fibres is being used for observations, the second set is being reconfigured for the next target field.

In order to give an unvignetted field of over 2° with a flat focal plane, a special corrector lens system had to be designed and manufactured (Taylor & Gray 1994).

Any wide-field multi-fibre system must be able to cope with two separate atmospheric refraction effects, the variable distortion of the field as the telescope tracks across the sky, and variation of

distortion with wavelength, which turns point images into very low-dispersion spectra as zenith distance increases.

The first effect means that for any one target field configuration, there is a maximum exposure time after which some of the target objects move out of the fixed fibre apertures. If we specify that a target field must be reconfigured once the target objects have moved more than a third of the fibre diameter (0.7 arcsec in the case of 2dF), this defines the maximum time available for the robotic positioner to reconfigure the next set of fibres. The effect of differential refraction is dependent on hour angle and declination as shown in Fig. 1. Evidently a reconfiguration time of at most an hour is required for an efficient system which can access most of the sky with minimal loss of observing time.

The second effect arises because the atmosphere is a refracting medium the refractive index of which depends on wavelength. For example, at a zenith distance of 60° , the light from a point source with wavelengths between 365 and 1100 nm is spread out over 4.2 arcsec, which would make it impossible to use 2-arcsec fibres for low-dispersion spectroscopy over a wide wavelength range. 2dF has an atmospheric dispersion compensator (ADC) built into the front two elements of the corrector. These two elements are slightly prismatic and are automatically counter-rotated during observations to provide an equal but opposite dispersion, to counteract the atmosphere as the telescope tracks across the sky.

The fibres feed a pair of spectrographs which are mounted at the top of the AAT near the prime focus, to keep the fibres short and maximize the UV throughput. Each spectrograph takes 200 spectra simultaneously, with resolutions of between 500 and 2000, on Tektronix 1024-pixel square CCD detectors. Mechanisms inside the spectrographs switch the fibre feeds in phase with the tumbling of the field plates.

All of the hardware making up the 2dF facility, including the spectrographs and electronics racks, is mounted on a purpose-built top end ring allowing straightforward interchange with the other three original alternative top ends of the AAT. In particular, the entire fibre system can be left assembled and available for maintenance when 2dF is not scheduled on the telescope.

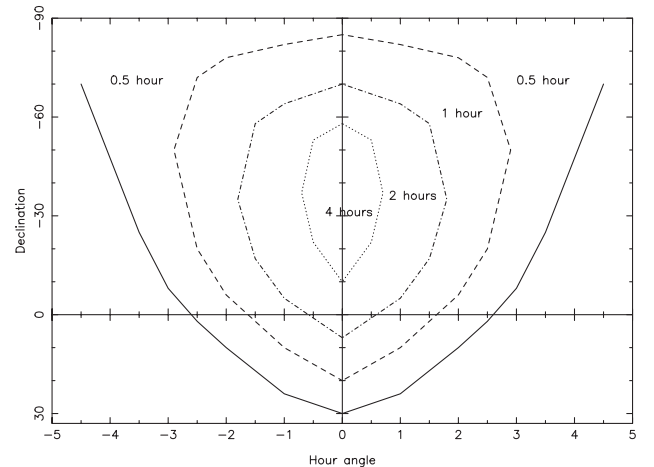


Figure 1. The effect of differential atmospheric refraction at the latitude of the AAT (-31°). The contours show the maximum possible observation times for 2dF fields centred at different hour angles and declinations, if all targets are to remain within one-third of a diameter of the centre of their fibres.

3 MAIN COMPONENTS OF 2dF

This section contains technical descriptions of the main components of the 2dF facility. At the end of this section Table 1 summarizes the main instrument properties.

3.1 Top end ring

The new 2dF top end ring (Fig. 2) is a direct copy of the three original AAT top end rings ($f/8$ and $f/15 + f/35$ secondaries and $f/3$ prime focus) (Sadler, Harrison & Lee 1991). This allows a fast (<1 h) interchange between top ends using the semi-automated mechanisms built into the AAT dome.

3.2 Design constraints on the prime-focus corrector

At the heart of the 2dF facility is the corrector lens system which provides the $2^{\circ}1$ diameter field of view at the AAT prime focus. The development of a corrector was initiated with a design by C. G. Wynne (Wynne 1989) offering a 2° field with 1.5-arcsec images using a four-element corrector. Further work by D. Jones and R. G. Bingham emphasized the need for an atmospheric dispersion compensator, the importance of chromatic variation in distortion (CVD) and of the telecentricity of the optical design. A relatively flat focal surface was also a requirement.

The atmospheric dispersion of uncorrected images when sampled with a small fixed aperture size (an optical fibre) will reduce the throughput of the system significantly, by an amount which varies strongly with wavelength and zenith distance. When combined with small positioning and astrometric errors this will place severe limits on the ability to flux calibrate the resulting data. In order to minimize this effect an atmospheric dispersion compensator built into the corrector optics must provide a variable amount of dispersion in the opposite direction to the atmospheric dispersion, for as large as possible a range of zenith distances.

All of the initial designs (except for a significantly aspheric design by Bingham) exhibited CVD to some extent. This effect causes off-axis, broadband images to be spread radially by up to

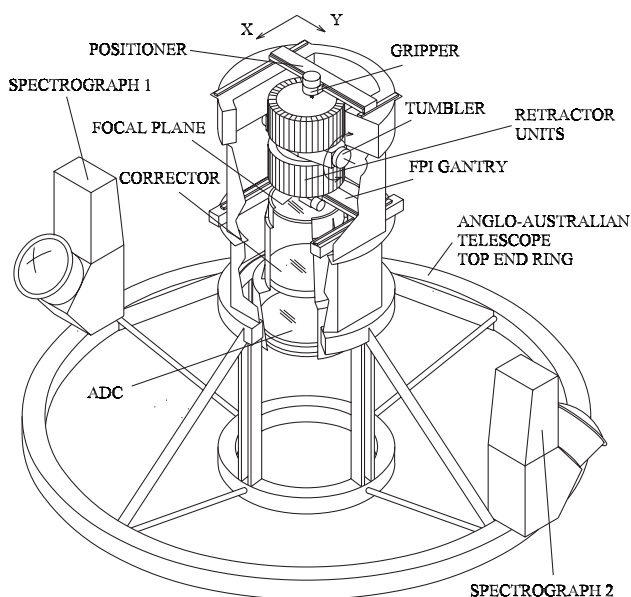


Figure 2. Schematic diagram of the 2dF top end showing the main components located on the mounting ring.

about 2arcsec for the 350–1000nm wavelength range, with maximum effect at about 0.5 field radius. This is a smaller effect than that of atmospheric dispersion and is independent of zenith distance; it determines the ultimate limit to spectrophotometric accuracy with 2dF.

The telecentricity of an optical corrector design defines how the principal ray of each cone of light reaches the focal plane of the telescope. For an ideal fibre system the principal ray should be orthogonal to the focal surface. If the input light cone is not perpendicular to the focal surface then even in the absence of fibre focal ratio degradation (FRD) the effective focal ratio of the output beam is decreased. In initial designs the angle of the principal ray varied across the field (usually increasing towards the edge of the field) by as much as 4° from the normal to the focal plane. This variation in input angle is effectively the same as reducing the input focal ratio of light to the fibre from $f/3.5$ to $f/2.3$. Note that this is a much more severe effect than that of FRD within the fibre itself, which is minimal when working at this input focal ratio.

If the spectrograph collimator is oversized to allow for this decrease in focal ratio, then we will reduce the spectral resolution

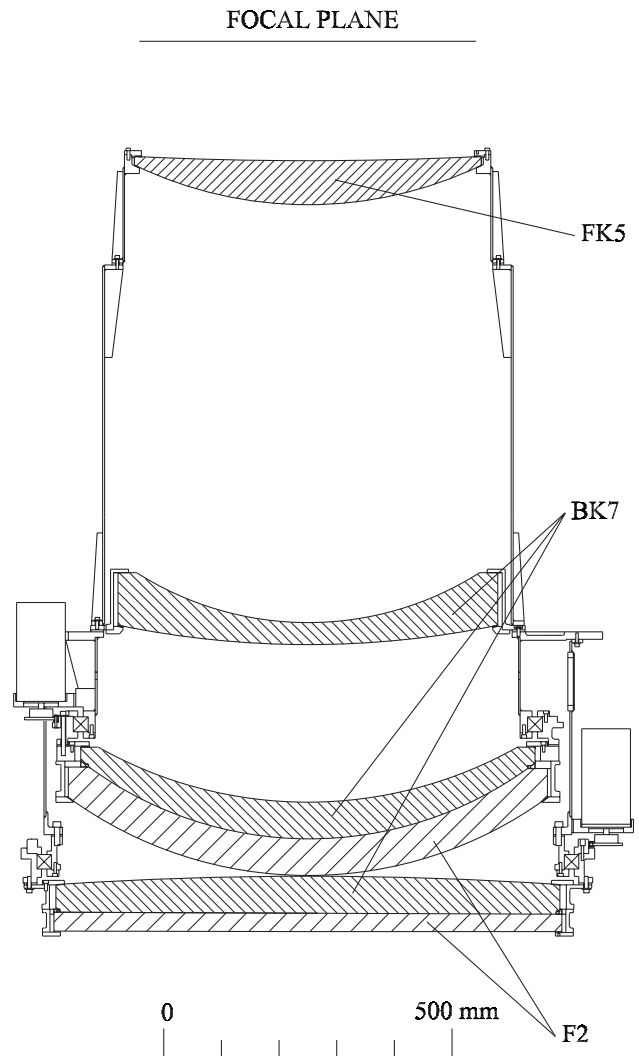


Figure 3. Schematic diagram of the 2dF prime-focus corrector in cross-section. The lower two lens elements are the prismatic doublets making up the ADC; these are the first and second elements of the corrector in the light path.

for a fixed spectrograph beamsize and camera focal ratio. Alternatively, if the collimator is sized correctly for the $f/3.5$ beam, fibres accepting light from near the edge of the field (the worst affected) will be severely vignetted. Unfortunately, the non-telecentricity of the final optical design means that the principal ray varies by up to 4° from the orthogonal case. This effect is partly compensated for in the design of the fibre probes (detailed in Section 3.4). A slight oversizing of the spectrograph collimator also reduces the effect of the non-telecentricity and any fibre FRD.

The design of corrector finally selected (Jones 1994) contains counter-rotating prismatic doublets as the first two lens elements (see Fig. 3). These provide atmospheric dispersion compensation for zenith distances of up to 67° . The prismatic lenses are designed to give zero deviation of the optical path. CVD is maintained below 1.0 arcsec across the field for the maximum bandpass used by the spectrographs. The CVD is zero at the centre and edges of the field and reaches its maximum value at 30-arcmin field radius.

The 2dF project is exceptional in that the scientific imperatives drove the design towards a large field and high multiplex advantage, while the fixed fibre size, realistic astrometric errors and relatively poor average site seeing (median value 1.5 arcsec) all reduce the importance of the absolute imaging performance of the corrector optics. In response to these criteria and the three design issues raised above, extensive system modelling was performed on the design (Taylor & Gray 1993). This allowed not only the quantitative assessment of performance issues, but also the evaluation of the cost and risk implications of each potential design as work proceeded.

3.3 Building the corrector lens

At 0.9-m diameter, the corrector optics contain some of the largest refracting elements made for an astronomical telescope.

The glass blanks for the corrector were manufactured by Ohara (Kanagawa, Japan). Since some of the corrector lenses are of a deep meniscus shape, a technique known as slumping was used to avoid a large and expensive wastage of glass and prolonged grinding. Instead of cutting a lens from a thick blank, a thinner glass blank was heated and allowed to soften and slump under gravity over a convex mould. This technique does have the risk of increased internal stress and hence variable refractive index within the slumped blank. Tests before and after slumping showed that any variations in refractive index were within specification.

The internal transmittance, particularly in the UV and blue, was also an important consideration in selection of the glass. The catalogue specification of UV and blue transmittance of BK7 and F2 glass types is significantly worse than that of UBK7 and LLF6 glass. However, discussions with the glass manufacturers revealed that the actual melt values were likely to be substantially better than the catalogue specification. Fig. 4 shows the corrector throughput using actual glass melt transmittance measurements, compared with the catalogue values for the glasses used in the 2dF corrector.

The glass blanks were figured, coated with a MgF_2 quarter-wavelength anti-reflection coating (optimized for 500 nm) and mounted by Contraves (Pittsburgh, USA).

The two ADC elements are prismatic doublet lenses with the BK7 and F2 elements in contact to reduce the number of air-glass surfaces. An optical coupling compound is used between each of the lenses making up the doublets.

After optical alignment in the corrector cells using temporary adjustment screws, the glass elements were mounted using flexible

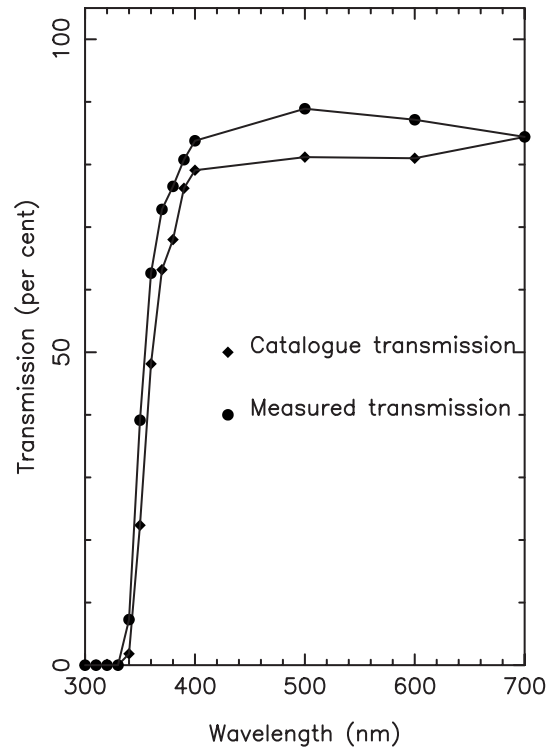


Figure 4. The wavelength dependence of the optical corrector transmission. This is based on measured and catalogue values of the bulk glass transmission and the predicted transmission of eight air-glass surfaces with quarter-wavelength MgF_2 anti-reflection coatings tuned for 500 nm. The actual transmission exceeds 80 per cent for wavelengths between 385 and 700 nm, falls to 60 per cent at 360 nm and is negligible below 340 nm.

silicone rubber which allows for the differential thermal expansion of the steel corrector housing and the glass.

The two lens elements that form the ADC are rotated using stepper motors. These automatically move the ADC elements to the required position whenever the telescope is slewed and then track continuously during observations. A mechanical switch acts as an index mark for each ADC element. Step counting is used to measure the position angle of the dispersing element. Each long slew of the ADC elements takes up to 3 min and includes a pass through the index marks to ensure that lost steps in the stepper motor do not accumulate and contribute to incorrect positioning of the lens elements.

The optical corrector was received from Contraves as a complete unit and commissioned on the AAT between 1993 July and October, by taking direct night sky images with photographic plates and both cooled and uncooled CCD detectors (Taylor & Gray 1994). These tests included verification of the broad-band imaging performance and the operation of the ADC, as well as the initial distortion mapping of the corrector and telescope optics.

3.4 Optical fibres and retractor units

The focal plane of the telescope is populated by a total of 404 deployable optical fibre probes which may be moved to cover any part of the available field of view of the corrector. The fibre probes are divided into two types: one for target objects and the other for guide stars. The 400 object fibres each consist of a single 8 m long optical fibre of core diameter 140 μm , corresponding to an average diameter of 2.1 arcsec on the sky (the effective diameter decreases

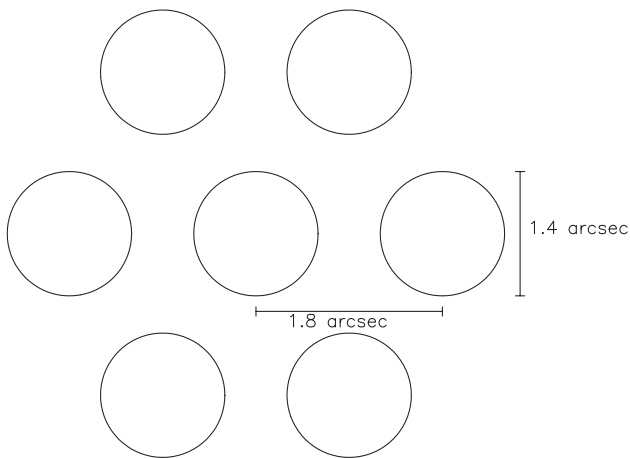


Figure 5. Fibre arrangement for a single guide fibre probe showing the arrangement of the seven individual optical fibres and their size and separation on the sky.

non-linearly from 2.16 arcsec at the field centre to 2.0 arcsec at the edge of the field). The four guide fibre bundles each consist of a 4-m long coherent bundle of $7 \times 100 \mu\text{m}$ core diameter fibres in which six fibres are arranged in a hexagon around a central fibre (Fig. 5). Each individual fibre probe can access an area extending from the edge of the focal plane to just beyond the centre of the focal plane, and can cover a sector with an apex angle of 28° . For the object fibre probes there is sufficient overlap between adjacent fibres to allow full field coverage. The four guide fibre bundles can access a total of about 30 per cent of the focal plane. The guide fibres are arranged at the four cardinal points on each fieldplate.

At the focal plane the incoming light is folded into the optical fibres using 92° prisms (1.2 mm on a side) made from Schott (Mainz, Germany) SF5 high refractive index glass, with the input face anti-reflection coated. The prism is glued to the polished end of the optical fibre using UV-curing cement, after being optically aligned with the fibre core. The 92° angle of the prism was chosen to be halfway between the extreme ranges of the beam angle for the non-telescopic corrector design. The prism material is a high refractive index glass so that the fast focal ratio input beam is totally internally reflected on the prism hypotenuse. This removes the requirement to aluminize the external reflecting face which would result in lower efficiency.

The optical fibre used is a high OH or wet fibre manufactured by Polymicro Technologies (Phoenix, AZ, USA). This has the advantage of good blue throughput at some cost of additional OH absorption bands in the far red (see Fig. 6). The optical fibre is a step index fibre with a core diameter of $140 \mu\text{m}$, a cladding diameter of $168 \mu\text{m}$ and a polyimide protective buffer $198 \mu\text{m}$ in diameter.

Each fibre and prism assembly is held in the focal plane by a small steel button 4 mm long and 2 mm wide containing a rare earth magnet (NdFeB) in its base (see Fig. 7). The magnet holds the button in place on a steel field plate located just behind the telescope focal plane. The button has a vertical fin or handle to allow the robotic gripper to grasp the button easily. Particular care was taken in the design of the button, with extensive simulations of the design to minimize the impact of the fibre probe footprint on the success rate with which fibres could be assigned to objects (Lewis et al. 1993). An overlarge fibre probe footprint would affect the success with which fibres could be assigned to target objects clustered on relatively small scales, thus potentially imposing an instrumental signature on the observations.

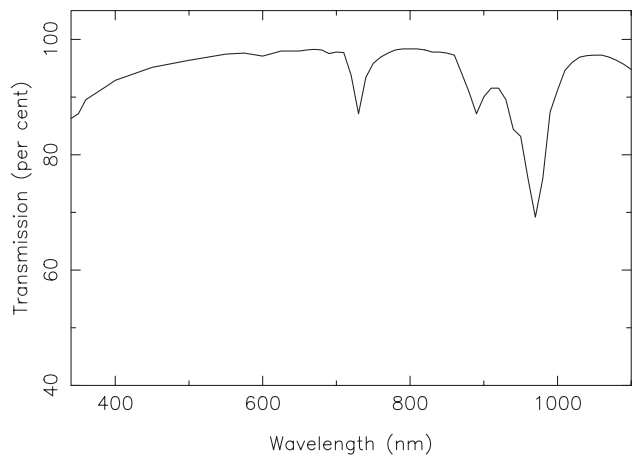


Figure 6. Optical fibre throughput as a function of wavelength (ignoring end losses). Fibre is Polymicro FVP 8 m in length.

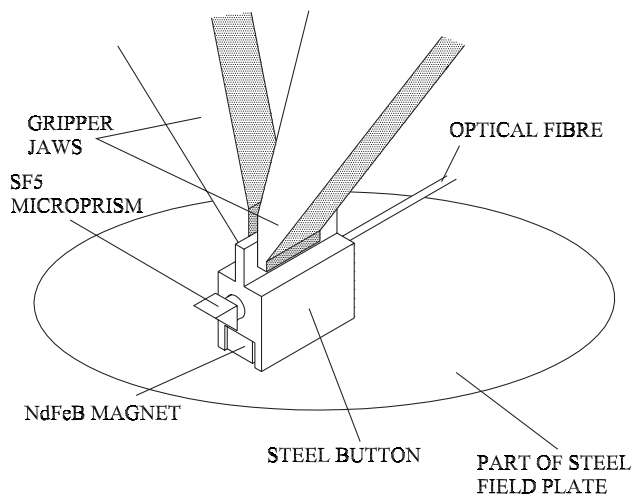


Figure 7. Diagram showing design of fibre probes and the gripper jaws.

The output ends of the optical fibres at the spectrograph slit are aligned together in multiples of 10 fibres which form a slitlet. The 10 fibres are aligned and cemented on to a brass block using an assembly jig to provide the necessary fibre-to-fibre separation. The fibre separation projects to 5 pixels at the detector. The brass block and optical fibres are then polished together as a unit. The slitlets are held in the focal plane of the spectrograph as a set of 20 slitlets to form the spectrograph ‘slit’ of 200 fibres. The fibres are fanned out to optimize the light path through the spectrograph optics.

Unlike previous AUTOFIB-type fibre positioners, the 2dF fibre probes do not have protective stainless steel tubes along their length in the focal plane area. These tubes had a number of uses: they protected the fibre against breakages, avoided any risk of fibre tangles and simplified the fibre allocation process. However, when the fibre probes are parked at the periphery of the focal plane, the steel tubes must be accommodated outside the fieldplate area which increases the overall size of the instrument. This was not a problem with previous Cassegrain focus instruments on the AAT, but would have led to loss of light at prime focus. A second disadvantage with steel tubes is that they severely restrict the use of fibre–fibre crossovers in the fibre allocation process, thus considerably limiting the number of fibres that can be allocated to target objects.

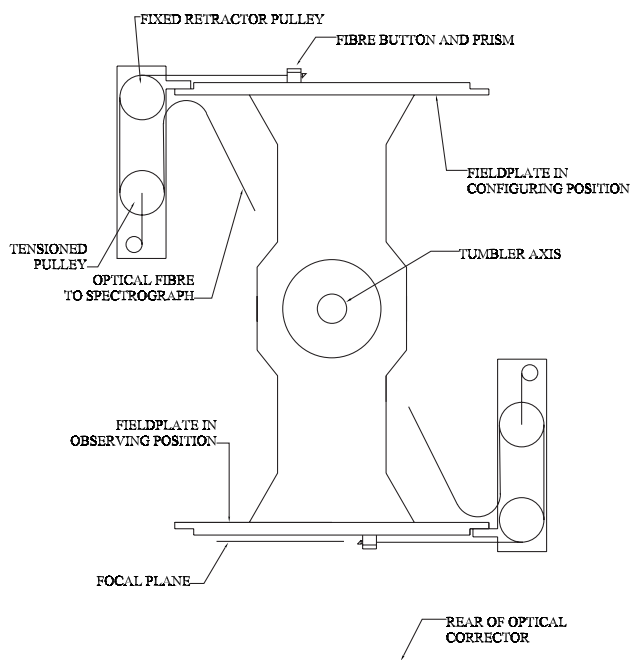


Figure 8. General arrangement of tumbler unit, fieldplates and fibre retractors. The drawing is deliberately not to scale to show detail; only one of 40 retractor units is shown on each fieldplate for clarity.

At the edge of the focal plane the fibres enter retractor units which keep the fibres straight on the fieldplate. Each fibre is mounted on a pair of pulleys within a retractor unit and independently maintained under 30-g tension using constant-force springs (Parry et al. 1993). After exiting from the retractor unit each bundle of 10 optical fibres is protected by a single PTFE tube and is routed through the tumbler rotation axis (see Fig. 8) and across the telescope top end ring spider vanes to the periphery of the top end ring where the spectrographs are located. The tumbler rotation axis is accommodated by allowing the fibres to twist.

Each retractor unit contains 10 fibres or 11 fibres (10 target fibres and a guide bundle for the four retractor units per plate that also carry a guide fibre bundle) to match the fibre slitlets. This allows for the exchange of a complete retractor unit for subsequent repair. A total of 40 retractor units are arranged around the circumference of each of the two fieldplates. This gives a total of 404 fibre probes on each of the fieldplates. 10 complete retractor units are maintained as spare units.

This system has the advantage of maintaining the fibres in a straight line between the button and edge of the focal plane without increasing the footprint of the fibre probe in the focal plane. A drawback is the complexity of the retractor units themselves and the high reliability required, since a failure of the retractor unit will cause a loop of slack fibre to protrude over the fieldplate which may lead to tangles.

An additional benefit of the bare fibre approach is that it is possible for each fibre to cross over many other fibres on its way from the edge of the focal plane to its target object. This considerably reduces the restrictions on allocating fibre probes to objects, at the cost of extra software to ensure that no attempt is ever made to move a button while its fibre is overlaid by other fibres.

3.5 Tumbler and fieldplates

The fibres are held in the focal plane of the telescope prime focus by magnetic buttons (as described in the previous section) on a flat

circular magnetic stainless steel fieldplate 560 mm in diameter. Two of these plates are arranged back to back on a tumbler arrangement (Fig. 8). The tumbler can be rotated back and forth through 180° to bring either fieldplate into play at the focal plane of the telescope. The other fieldplate is then ready to be accessed by the robotic fibre positioner.

Embedded in each fieldplate are 21 reference marks in a regular grid pattern. These reference marks consist of polished optical fibres inserted into holes in the fieldplate. The other ends of the optical fibres are illuminated by light emitting diodes (LEDs). These reference marks have accurately known positions within the fieldplate and are the primary reference frame for both the gripper and focal-plane imager gantry coordinate systems. The use of polished optical fibres means that the gripper optics can image and centroid the reference marks reliably.

3.6 Robotic positioner

A single fast robotic positioner (Smith & Lankshear 1998) is used to manipulate the individual optical fibre probes. Once the robot is given a list of X , Y positions (converted from astronomical coordinates provided by the observer), the positioner control software works out an optimal way to reconfigure the fibres from their current locations to the required positions. This usually requires moving a number of the fibres out of the way (i.e. parking them at the periphery of the field) before moving the majority of the fibres directly to their target position. This is at least 50 per cent faster than the more simplistic approach of parking all of the fibres before moving each fibre to its new target position.

The robot consists of a complex gripper unit mounted on an X - Y Cartesian gantry, mounted above the tumbler fieldplate at the top of the 2dF central section (Fig. 2). The gripper gantry has two X -axes and a Y -axis cross-beam in an ‘H’ configuration. The axes are driven by linear AC servo motors. The use of linear motors over the more conventional leadscrews allows faster and more accurate motor control and eliminates the effects of backlash. Positional information is determined from independent linear optical encoders for each axis, with a resolution of 1.25 μm .

All movements of the X - Y gantry are balanced by counterweights that move in the opposite direction to the gantry, resulting in zero net momentum at the prime focus when the positioner is operational. With these precautions there is no measureable effect on the tracking of the telescope arising from the movement of the gripper gantry during observations.

The gripper unit contains a rotational θ -axis to allow the gripper to be aligned with the (approximately radially aligned) off-axis button handle, a Z -axis to raise and lower the gripper unit and a set of jaws to grasp the individual button handles. The handling of the fibre probes is monitored by a small video CCD camera and optics built into the gripper unit. The optical fibres are back-illuminated by light projected into the optical fibre from the spectrographs. The robotic positioner can ‘see’ the illuminated end of the fibre and knows the physical offset to the button handle which it grasps. This system allows the gripper to monitor fibre placement at the new target position, measure any positioning errors and if necessary correct those errors if they are deemed to be too large (Lewis & Parry 1990; Parry et al. 1993). This has the advantage that the robot positions the fibre core at the required position regardless of any actual manufacturing or assembly errors in the fibre button assembly. Note that for the guide fibre bundles only the central fibre in the coherent bundle of seven fibres is back-illuminated during the positioning process.

The gripper unit was built under contract by the University of Durham to an AAO design, following earlier development work for the initial 2dF design study.

The design of the gripper jaws used in this process is particularly important and went through several prototyping stages (Wilcox 1993) in order to achieve repeatability at a level better than the overall accuracy requirements. One of the pair of gripper jaws is fixed to the $X-Y-\theta$ gantry and forms a reference surface while the second jaw is movable. To grasp a fibre button the fixed jaw is positioned against the button handle using the $X-Y-\theta$ gantry, then the movable jaw is closed on to the handle to avoid knocking the fibre button unnecessarily. Releasing the button requires the movable jaw to be moved away from the button handle slightly before the fixed jaw is backed away from the button handle using the $X-Y-\theta$ gantry.

The robotic positioner is capable of configuring a full target field of 404 fibres in about an hour. This requires on average a total of 600 fibre movements to untangle the previous field and configure the new target field, at a speed of under 6 s per move. The average positioning error is $11\ \mu\text{m}$ (0.16 arcsec) with all fibres required to be placed within $20\ \mu\text{m}$ (0.3 arcsec) of the demanded position; if necessary, the robot picks up and replaces the button until the position is within tolerance.

The effect of any offset arising from flexure between the gripper gantry and fieldplate is removed using the grid of reference marks embedded in each fieldplate. These are measured with the gripper CCD video camera before positioning the fibres on the fieldplate. This survey process is always performed after a tumble operation or after the telescope has been slewed to a new position, before any fibres are moved.

3.7 Fibre spectrographs

With a fibre-linked spectrograph one has to balance the merits of using long fibres to feed a remotely located bench spectrograph, against using very short fibres and mounting the spectrographs close to the fibre positioner. Each approach has its merits and drawbacks. The remotely mounted spectrograph has the advantage of providing a stable spectrograph and making the engineering much simpler, but with the drawback of the lower UV throughput of long optical fibres (30 m). Using short fibres with a locally mounted spectrograph reduces the UV light losses caused by the fibre length but increases the mechanical design difficulties and subjects the spectrograph to variable gravitational flexure, and ambient temperature variations, as the telescope tracks across the sky.

The choice between a single monolithic spectrograph accepting all 400 optical fibres, and a pair of smaller spectrographs each accepting 200 optical fibres was largely determined by the availability of Tektronix 1024-pixel square CCD detectors. These limit each detector to 200 fibres spaced by 5 pixels on the detector. Larger detectors were promised but not available during the predicted time frame of the instrument construction. Limiting each spectrograph to 200 fibres also eased the optical design somewhat, since it required a shorter slit assembly.

The decision was made to keep the fibre lengths as short as practicable by locating the spectrographs at the top end of the telescope (Smith & Lankshear 1998). Initially they were to be mounted above the robot positioner (Taylor & Gray 1990) with an extremely short fibre length. The final design, however, was constrained by the available space envelope and the spectrographs

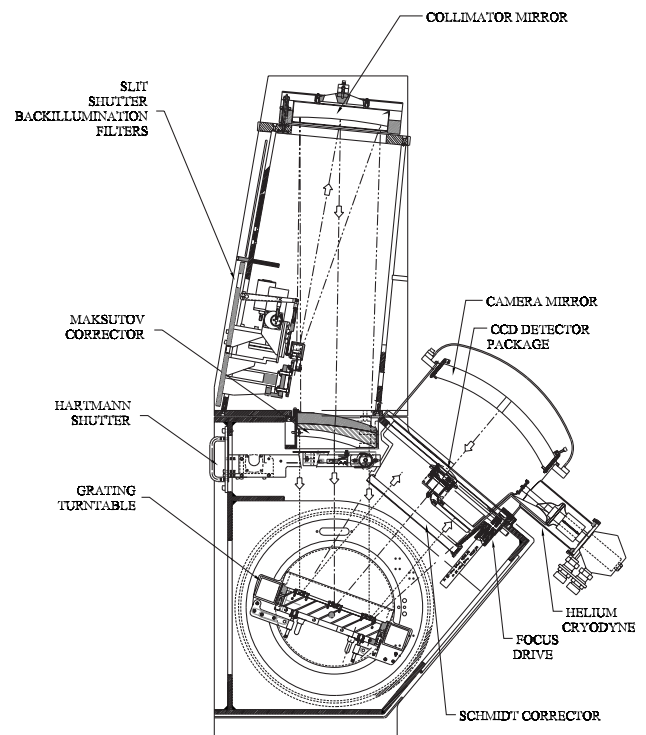


Figure 9. Spectrograph general arrangement showing the main components and the optical path.

were mounted at the edge of the top end ring as shown in Fig. 2. This resulted in a fibre length of 8 m.

The overall construction of the spectrographs is depicted in Fig. 9. The spectrograph design is based on an $f/3.15$ off-axis Maksutov collimator generating a 150-mm beam. This allows the use of the existing 150×200 mm Cassegrain Royal Greenwich Observatory (RGO) spectrograph reflection gratings. The collimator is slightly oversized compared with the prime-focus corrector focal ratio of $f/3.5$, to allow for some focal ratio degradation in the optical fibres and further reduce any effect of the non-telescopicity of the corrector design. The off-axis design has the benefit of no central obstruction so the fibre slit and its associated shutter, filter wheels and slit interchange mechanism do not vignette the beam.

The 200 optical fibres from the focal plane are arranged in a single line to form a pseudo-slit. A shutter is located immediately in front of the fibre slit. The shutter is moved in a direction perpendicular to the slit axis and therefore only requires a short travel to open and close over the slit width as defined by the fibre diameter of $140\ \mu\text{m}$.

Two filter wheels, each with four apertures, are provided behind the shutter. One aperture in each filter wheel is kept as a clear aperture leaving a maximum of six filter spaces of which three are currently used to hold order-sorting filters for high-resolution observations. The filters themselves are 2 mm thick. Filters currently available include GG495, S8612 and RG630. Use of a filter requires a change in the spectrograph focus as the filters are located in the diverging beam behind the fibre slit and shutter.

The spectrograph camera is located at a collimator-camera angle of 40° and is a fast, wide-field Schmidt camera with a CCD at its internal focus (Jones 1993). The main difficulty with the camera is that the pixel matching requirements of imaging such a large number of fibres on to such a small detector force it to have an f -ratio as fast as $f/1.2$ in the spatial direction ($f/1.0$ in the spectral

direction) while retaining its wide $\pm 5.5^\circ$ field of view. The camera uses a severely aspheric front corrector plate, to give good performance over the full wavelength range and field angle required to image the spectra.

The camera is fully evacuated with the aspheric Schmidt corrector lens acting as a dewar window. Each CCD is cooled by use of a cold finger attached to a CTI Cryogenics (Mansfield, MA, USA) closed-cycle helium cooler. A helium compressor is mounted on the telescope in a gymbal mount and is used to drive both cryodynes. The cool-down time for the CCDs is relatively long, about 3.5 hours from ambient temperature to their operating temperature of 170 K. The performance of the cryostats is sufficiently high to maintain their performance for up to 21 days.

In addition to the basic design of the spectrographs, the double buffering of the fibre positioner system and the back-illumination of the fibres provide some extra engineering problems. Each spectrograph actually accepts 400 fibres, 200 from each field plate, which must be located in the focal plane of the spectrograph when required. The non-observing fibres must be illuminated with a light source bright enough to be seen by the gripper TV system of the robotic positioner since fibre positioning is done simultaneously with observing. These two requirements mean that each spectrograph must have a slit interchange mechanism, a bright light source for the fibre back-illumination, and a reliable means of completely shielding this light source from the rest of the optical path.

The spectrograph is focused by moving the detector within the cryogenic camera. Both focus and tilt adjustments of the CCD are available and can be driven remotely.

With the exception of the selection of the grating (which has to be manually inserted before observations start), all functions of the spectrographs are remotely controlled. This includes slit change-over, filters, Hartmann shutter, grating rotation and spectrograph focus. Gratings can be automatically recognized by the spectrograph control system which reads magnetic barcodes present on all of the grating cells.

The complete spectrograph configuration is inserted into the data FITS header information to allow automatic pipeline data reduction.

3.8 Focal-plane imager

A second X - Y gantry, almost identical to the gripper gantry, is located immediately behind the final element of the optical corrector (Fig. 2) and in front of the observing fieldplate. Instead of a gripper unit, this gantry carries a pair of CCD cameras. One camera is a simple video CCD camera which can only view the back-illuminated fibres and field plate, while the second is a Peltier cooled Princeton Instruments (Trenton, NJ, USA) CCD camera, facing in the opposite direction, which can view the sky when its gantry is appropriately positioned. This gantry system is known as the Focal Plane Imaging (FPI) system and is the primary means of determining the relationship between RA, Dec. and X , Y on the fieldplates. This sky viewing camera can also be used for target field acquisition and seeing measurements. The image scale of the focal-plane imager CCD is 0.3 arcsec per pixel.

The focal-plane imager gantry also surveys the reference marks embedded in the field plates, in a similar manner to the gripper gantry, to correct for registration and flexure before centroiding the images of reference stars.

3.9 Calibration systems

2dF contains its own remotely controlled calibration systems. Two

white flaps may be inserted into the telescope beam below the corrector, blocking off sky light and forming a reflective screen. A variety of calibration lamps can be used to illuminate this screen, with the resulting scattered light travelling through the 2dF corrector and illuminating the focal plane. Two intensities of quartz lamps for fibre flats and a variety of hollow cathode arc lamps (copper–argon, copper–helium and iron–argon) are provided.

Requesting an arc or fibre flat exposure will result in the control system automatically inserting the reflective flaps and turning on the requested calibration lamps. At the end of the exposure the lamps are turned off and the flaps either removed from the telescope beam or left in place if further calibration exposures are required. This automation avoids accidentally leaving calibration lamps turned on and reduces observing overheads.

All calibration exposures have appropriate FITS header items added to the data frames as an aid to the pipeline reduction of the data.

3.10 Software control systems

The 2dF facility uses the AAO DRAMA software infrastructure (Farrell, Bailey & Shorridge 1995) to build a fully integrated control system across several computers and operating systems.

The graphical user interface is written using TCL/TK and provides for control of all aspects of the positioner system, the spectrographs, ADC and CCD control, all from one simple-to-use interface. The same interface allows the observer to control the telescope directly, for example when slewing to a new target field. The graphical user interface is provided by several windows spread across two computer screens with controls arranged by subsystem.

Individual parts of the 2dF facility are controlled by software tasks which are running on the most appropriate control computer (VxWorks, Solaris, VMS), and DRAMA allows the many separate tasks to communicate and work together seamlessly.

3.11 CCD operation

The two Tektronix 1024 CCDs are controlled using the standard AAO controller hardware, the AAO External Memory (XMEM) and OBSERVER software interface on a VAX/VMS computer system. With a slight adaptation, the OBSERVER software communicates with the rest of the 2dF control system (running on Solaris and VxWorks computer systems) using DRAMA to enable it to add all of the more specialized 2dF FITS header items from the 2dF control system to the data files for archiving. The two CCDs are operated and read out simultaneously, but using separate controllers and data links.

3.12 Acquisition and guiding systems

On each fieldplate there are four guide fibre bundles which do not feed to the spectrographs. These guide fibres consist of a coherent bundle of seven individual fibres with six fibres in a hexagon pattern surrounding a central fibre (Fig. 5). The separation of the individual fibres in a guide bundle at the input end is 1.8 arcsec. Each guide bundle may be positioned on a guide star in the focal plane to allow for acquisition of the target field. The output from the four guide fibre bundles is collected by an intensified camera TV system, with its output visible to the telescope night assistant and observer. A guide star is accurately centred when the central fibre of a guide fibre appears brightest on the TV display and the six surrounding fibres are uniformly illuminated.

A minimum of two guide fibres are recommended for each target field, although it is preferable that all four are used in case of inaccurate stellar positions. The Quantex TV system can detect stars down to a magnitude limit of $V = 15.5$ in average conditions. The system was designed to include an option to rotate the fieldplates for target acquisition and, if necessary, during tracking. However, this has not yet been implemented. It turns out that the instrument is sufficiently stable, and the flexure is small and predictable, so that it is easier to remove any overall field rotation in the positioner software. Often, larger errors would be introduced by attempting to use the fiducial stars to correct rotation, especially since the surface density of usable stars means that it is difficult to obtain enough stars close to the edge of the field to allow rotation to be determined.

The pointing of the AAT is normally good enough (better than 2 arcsec) that target field acquisition is a simple procedure of slewing the telescope and the guide stars will be visible somewhere in at least one of the guide fibres. Fine acquisition is performed manually by offsetting the telescope by very small amounts until all four guide stars are well centred in their respective guide fibres.

If for any reason the guide stars cannot be seen after slewing the telescope or there is any ambiguity in the guide star acquisition (for example because of a very crowded field in a globular cluster or poor guide star positions), the focal-plane imager CCD camera can be used to image a small section of sky around each guide star to verify acquisition. A simple offset will then place the guide stars on to the guide bundles, after which the focal-plane imager can be removed from the focal plane.

Once a target field is acquired, guiding can be done in one of two ways. The normal guiding method is manual guiding using the excellent tracking of the AAT and making small adjustments every 10 min or so.

An automatic autoguider has also been developed which uses the video output from the Quantex TV system to feed a video frame grabber. The digitized video can then be analysed to determine the average centroid of each guide fibre and determine the correct telescope offset to restore the telescope pointing. Initially, however, the extra calibration required and problems with the dimensional stability of the Quantex TV image at different gain levels meant that autoguiding was not generally used. A simplified version of the autoguider system was implemented in 2001 under the control of the telescope night assistant, and this is now in regular use.

4 OPERATION OF 2dF

4.1 Input data, astrometry and guide stars

The successful operation of a robotic fibre system depends on the provision of accurate positions for the target objects in a known reference frame. Target positions are usually measured from Schmidt telescope photographic plates, using the Automatic Plate Measuring (APM) or SuperCOSMOS plate measuring machines, although more recently astrometry from CCD mosaics is becoming more common and reliable. With care, these provide astronomical coordinates with a relative accuracy of 0.2–0.3 arcsec across the full 2° field of 2dF. This involves using a reliable modern

Table 1. Summary of 2dF instrument specifications.

Telescope	3.9-m AAT $f/3.3$ Prime focus
Corrector field of view	$2^\circ 1$
Corrector focal ratio	$f/3.5$
ADC recommissioned	1999 August 31
Image scale	$67 \mu\text{m arcsec}^{-1}$
Number of spectroscopic fibres	400 (on each fieldplate)
Number of guide fibres	4 (on each fieldplate)
Fibre diameter	$140 \mu\text{m}$
Fibre size on sky (mean)	2.1 arcsec
Reconfiguration time	55 min (typical)
Fieldplate exchange and acquisition	3 min (typical)
Robot positioning accuracy	$11 \mu\text{m}$ (mean) $20 \mu\text{m}$ (maximum)
Overall positioning accuracy	0.3 arcsec rms
Length of fibres	8.0 m
Spectrograph collimator	$f/3.15$ Off-axis Maksutov 150-mm beamsize
Spectrograph camera	Modified Schmidt camera $f/1.2$ (spatial) $f/1.0$ (spectral)
Detector	Tektronix 1024×1024 pixel CCD
CCD inverse gain (NORMAL and SLOW)	$2.79 - 1.4 e^- \text{ADU}^{-1}$
CCD readout times	74–120 s
CCD readout noise	$5.2 - 3.6 e^-$
Pixel size	$24 \mu\text{m}$
Second science grade CCD installed	1999 August 31
Dispersive elements	Plane ruled reflection gratings 205×152 mm
Range of available dispersions	4.8 to $1.1 \text{ \AA pixel}^{-1}$
Range of effective resolutions	9 to 2.2 \AA
Achievable velocity accuracy ¹	10 km s^{-1}
Spacing of spectra at detector	5 pixels
Fibre size at detector	1.9–2.1 pixels
Order sorting filters	GG495, RG630, S8612
Number of spectra/spectrograph	200
System throughput ²	5 per cent
Minimum object separation in focal plane	2.0 mm (approximately 30 arcsec)

¹ This is a typical external accuracy for the 1200 lines per mm gratings and is very dependent on the spectral type of the data.

² Total system throughput including atmosphere and telescope at 600 nm with 300B gratings.

astrometric catalogue of reference stars and taking full account of proper motions.

To place optical fibres on target objects, 2dF needs to know the conversion from astronomical coordinates to physical coordinates in the focal plane. This conversion is determined by measuring the fiducial marks on the fieldplates using the FPI TV camera, then measuring the X – Y positions of sets of astrometric standard stars using the FPI CCD camera. The observed centroids of the star images are matched to their expected positions, as corrected for atmospheric refraction, known telescope pointing errors and the distortion introduced by the 2dF corrector lens. A least-squares minimization determines the fitting parameters; the six free parameters are the scales in X and Y , the overall rotation and skewness of the field, and any offset of the centre of the optical distortion pattern from the optical axis. Any non-perpendicularity of the axes of the gantries, or mechanical shifts between the gantries and the fieldplates, should be automatically removed by the survey of the fiducial reference points on the fieldplates (Section 3.8).

For calibrating 2dF it was not a trivial task to find astrometric data with the required accuracy (current rms positions to better than 0.25 arcsec across 2° of sky) for large enough samples of stars. Initially, the Positions and Proper Motions (PPM) catalogue was used (Roesser & Bastian 1988); currently the *Tycho-2* catalogue (Høg et al. 2000) is the most suitable. Originally the astrometric calibration involved taking data for sets of stars at a range of declinations, for both field plates, and the full process had to be repeated on the first night of every 2dF observing run. Different sets of astrometric parameters were stored and used as appropriate for each target field. However, it appears that the behaviour of 2dF is sufficiently stable and repeatable that the flexure terms can be predicted. All that is now needed is to take at least one set of calibration data whenever 2dF is re-mounted on the telescope, to determine any rotation or offset zero-point errors. There are also small plate scale variations which are temperature-dependent. The remaining errors in the process should be below the 0.5-arcsec level at the edge of the field, where most effects are worst.

The fiducial or guide star positions should be as accurate as the target object positions and on the same astrometric system. However, for a number of reasons this may not be the case. First, fiducial stars are usually in the magnitude range $V = 13$ – 15.5 so that the Quantex TV system is able to detect them. Stars as bright as this can suffer haloes and diffraction spikes on the photographic plates which affect their astrometry. Secondly, proper motions of stars can increase the positional errors, particularly when using old plates. Using fiducial stars towards the faint end of the available range, restricting the colour range and comparing two plates of different epochs can reduce both these effects. A good solution is to use stars drawn from the target object list, where feasible. Alternatively, a prescription for the selection of guide stars is given by Colless et al. (2001).

4.2 Fibre allocation procedures

Fibres are allocated to target objects using an off-line software program `CONFIGURE` (see the 2dF WWW pages <http://www.aao.gov.au/2df/> for details of manuals and to download this software) to pre-plan each target field. An example target field configuration is shown in Fig. 10, which is a reproduction of the mimic display at the telescope. When provided with a field centre and a list of target, fiducial star and blank sky positions, the `CONFIGURE` program assigns fibres to objects, taking account of the hardware constraints (limited fibre extension and deviation from the radial direction) and avoiding illegal hardware collisions. Given the size and shape of

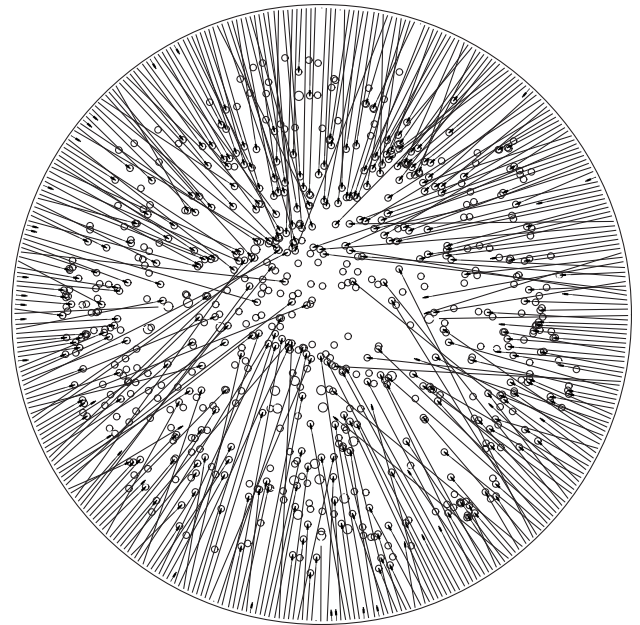


Figure 10. An example target field configuration using almost all 400 fibre probes. Unallocated target objects are shown by unfilled circles. A few fibres remain parked at the edge of the field because they cannot access any of the unallocated targets. Small circles represent targets and large circles are potential guide stars. Fibres apparently on blank areas have been allocated to sky positions.

the fibre buttons, the minimum separation between two targets is ≈ 30 arcsec on the sky, but this is a strong function of location in the field and of target distribution.

Various options in `CONFIGURE` allow the user to assign relative priorities to targets and set other parameters, including the planned hour angle of the observations, in order to optimize the allocation of fibres. The program works iteratively making a number of random swaps at each iteration to try to maximize the number of observable targets and minimize the number of fibre crossovers. The `CONFIGURE` utility includes an option for automatic allocation of fibres to sky positions and allows manual editing of the final fibre configuration, before saving as a file to be used with the 2dF control system at a later stage. One (or more, if the same field is to be tracked for several hours) of these configuration files is required for each target field to be observed during the course of a night.

If the user wishes to observe a field with more than 400 targets, the input list must be split into a series of manageable field configurations. It is usually best to restrict the magnitude range of targets in a given field, since bright targets may become saturated or scatter light on to fainter targets in adjacent fibres in the spectrographs.

To cover efficiently an area larger than the 2° field of view with high completeness requires simultaneous configuration of multiple fields and adjustment of their field centres; this process is known as ‘tiling’. A description of the tiling procedure used in the 2dF Galaxy Redshift Survey is given by Colless et al. (2001).

The off-line planning process is usually done well in advance and a set of configuration files sent to the telescope. Before a set of configuration files are used they are normally checked for legality using the current astrometric parameters.

4.3 Observing procedures

This section describes the standard observing procedure as used for

the major redshift surveys, although many of the steps are similar for all 2dF programmes. Observing with 2dF is somewhat different from most other observing on the AAT. The corollary to the complexity of the instrument, and the need for a great deal of preparatory work before coming to the telescope, is that it is difficult to make significant changes to the programme during the night. Thus there is usually little scope for interactive decision-making by the observers.

Another fundamental constraint is the fact that it is necessary to keep planning ahead, since the configuring of a set of targets takes about one hour, about the same as the time needed for one set of observations for the redshift surveys. Thus the observing and re-configuring have to be carried out simultaneously and almost continuously, so that any time lost in one aspect will lead to problems in the other. Not only that, but also the fibres have to be configured for the expected mean hour angle of the observations to minimize atmospheric refraction losses. One consequence is that if a set of observations is delayed for any reason, it is rarely possible to catch up; the best strategy is to abandon that set and move on to the next set. Having two fieldplates also introduces extra constraints: in the case of the redshift surveys, the configurations for each field are prepared for one or other specific fieldplate. Thus if one field is lost, it is not possible simply to move on to the next one; quite often the consequence of losing one field is an overall loss of two hours of observing, since the target configurations that have been prepared are no longer the appropriate ones.

The solution to these constraints is to prepare a detailed observing plan for each night. This plan must include all necessary exposures, including calibrations, with realistic estimates of the necessary elapsed time for each operation.

Before observing starts, and usually well before sunset, the first two configurations of the night have their fibres set up on the two fieldplates. Depending on the declination and hour angle, and on the distribution of targets (centrally concentrated fields can be observed over a much wider range of hour angle), a target field may have to be observed with multiple configurations to remove atmospheric refraction effects, as demonstrated in Fig. 1.

For each target field a minimum set of CCD exposures consists of a fibre flat (quartz lamp) exposure, an arc exposure and a set of target object exposures. The fibre flat is used for locating the spectra on the CCD during the data reduction stage; the arc exposure is for wavelength calibration of the spectra. Optional CCD exposures may include offset sky exposures and twilight sky flat exposures, both used for calibrating the fibre-to-fibre throughput variation.

If these special exposures are not taken, the fibre-to-fibre throughput calibration can often be done using the night sky emission lines in the object data frames; in fact, there is evidence that this method actually gives the best results, since the calibration data are simultaneous with the observations, use exactly the same optical path and do not involve moving the telescope. The night sky line method works best in the near-infrared part of the spectrum which has many emission features, or when particularly strong night sky lines are present, such as [O I] at 5577 and 6300 Å (Bailey et al. 2002).

Between target fields, the fieldplates must be exchanged using the tumbler, and the telescope and dome must be slewed to the new target field position. The ADC automatically tracks the telescope position, thus removing this complication for the observer. A straight-forward field changeover takes under 3 min. Once the telescope is tracking at the new target field location the robot positioner can start moving the fibres for the subsequent target field.

Observations of single standard stars (radial velocity standards,

metallicity standards etc.) are possible without reconfiguring all of the fibres. A calculation tool is provided to allow blind offsetting of a standard star into a single spectroscopic fibre, using a nearby guide fibre. This process is, however, not suitable for observing flux standards, owing to the uncertain nature of the final blind offset and the small size of the fibre aperture.

It is not yet clear how accurately it is possible to calibrate the fluxes in 2dF spectra, especially when taken over a wide wavelength range. Absolute fluxes can never be very accurate, since the fibre diameters (2 arcsec) are comparable to the typical ‘seeing’ disc size, and the overall accuracy of fibre positioning is often no better than 0.5 arcsec. Relative fluxes, i.e. as a function of wavelength, can be determined to higher precision. However, here the CVD inherent in the 2dF corrector lens (see Section 3.2) limits the accuracy attainable. Repeatable results should be obtainable for stars near the field centre, where the CVD is small, but over most of the field the combination of fibre positioning errors, CVD and variable seeing means that the slope of stellar spectra varies substantially, even between consecutive short exposures (Cannon 2000).

4.4 Data reduction software

During the design stages of 2dF it was clear that a dedicated pipeline data reduction package would be required to deal with the enormous amounts of data, up to 3000 spectra, which 2dF would be capable of generating during a single night.

A completely new data reduction software package (2DFDR) has been developed for 2dF (Taylor et al. 1996a; Bailey et al. 2002). The design philosophy of the 2DFDR package is to make as much use of known instrumental parameters as possible. In particular, 2DFDR uses the known optical properties of the spectrographs to predict the format of the data (location of the spectra and dispersion). The FITS headers of the data contain all the information needed to identify the different types of data frame, the location of all the target objects, details of the telescope and spectrograph parameters, and the appropriate calibration frames to be associated with each data frame. The 2DFDR package preserves the integrity of the data headers, together with the statistical variance of each spectrum and the sky spectrum that was associated with each object.

The 2DFDR program can be run automatically and is able to reduce the data from an entire night in an hour or less. However, it is normally better to do at least some of the steps interactively, especially the initial determination of the ‘tramline’ extraction maps for the spectra, and to verify that the results are sensible at each stage. The software package provides several options and many parameters that can be set, and includes a number of diagnostics for assessing data quality.

The data for a particular target field are reduced as two separate sets of data, one for each spectrograph containing 200 individual spectra. For the large redshift surveys, it is normal procedure to analyse the data as the night proceeds, with all observations fully reduced and all redshifts determined by the end of the night’s observing.

The data reduction software package 2DFDR is available for download from the 2dF WWW pages (<http://www.aao.gov.au/2df/>).

5 PERFORMANCE OF 2dF

5.1 Corrector optics

The initial imaging tests (Taylor & Gray 1994) showed that the 2dF

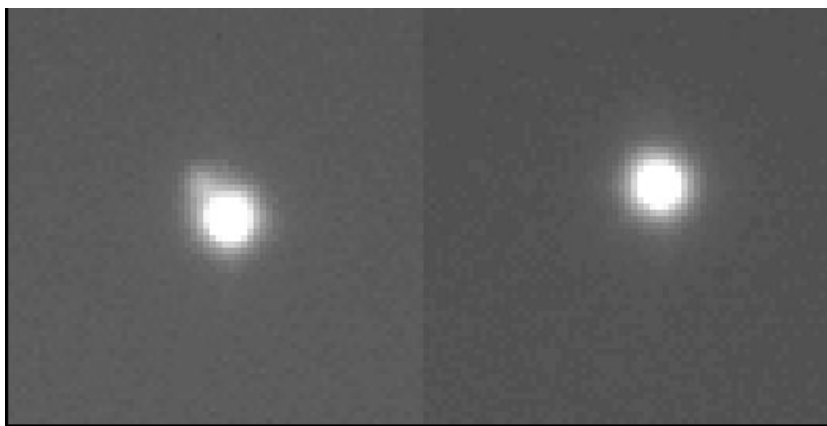


Figure 11. Operation of the ADC at 67° zenith distance. The left-hand image shows the image quality with the ADC nulled; the right-hand image shows the same stellar image with the ADC tracking at the appropriate orientation. Both images were taken in 1.5-arcsec seeing. The left-hand image shows the faint UV stellar image offset to the upper left of the brighter red image. Each image is 66 pixels (20 arcsec) on a side.

corrector lens optics met their design specification. The imaging performance was also checked in 2001 May, after some evidence of apparently variable throughput across the 2dF field (see Section 5.6 below). A series of spectra of a set of standard stars was taken, stepping through focus between exposures. These were somewhat inconclusive, given the fibre diameter of 2 arcsec and the sensitivity to ‘seeing’ variations. A better check was provided by taking a series of exposures on a sheet of photographic film, stuck on a sheet of magnetic material which was then mounted on one of the field plates. These showed that the focus is constant across the 2dF field to within $30\ \mu\text{m}$; there is no tilt of the focal surface and no serious variations in point spread function across the full field.

5.2 Atmospheric dispersion compensator

The effectiveness of the ADC has been demonstrated using the focal-plane imager CCD camera to take an image of a star at a zenith distance of 67° . A filter glass (Schott BG1) was inserted in the optical path which absorbs the visible light and passes UV and near-infrared. The results are shown in Fig. 11. The image taken with the ADC nulled (no correction of atmospheric dispersion) shows a slight separation of the UV and near-infrared images; the image taken with the ADC operating shows a circular superimposed set of images.

The ADC was shown to work well for imaging during the corrector lens acceptance tests in 1993. For these tests the ADC elements were manually driven to the correct position. However, later checks on the spectra of some bright stars at large zenith distance revealed a decrease instead of an increase in UV flux when the ADC was activated. This turned out to be due to a combination of software and zero-point errors in driving the two counter-rotating elements of the ADC. Since the pointing and guiding of 2dF are done at an effective wavelength of about 500 nm, this means that all low-dispersion 2dF spectra taken up until 1999 August are liable to have been degraded by an effectively random loss of UV and (to a much lesser extent) near-infrared flux, even for fields observed near the zenith. The effect is less serious for most high-dispersion spectra since they cover a shorter wavelength range. This problem was corrected in 1999 August and all subsequent data have the ADC operating correctly.

Direct tests on stellar spectra confirm the effectiveness of the ADC, which can increase the UV throughput by factors of 3 or more (Cannon 2000). Fig. 12 shows the ratio of two consecutive

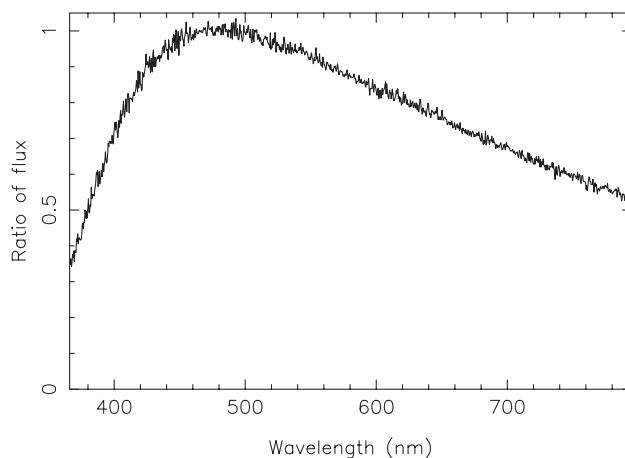


Figure 12. The ratio of two spectra of a star observed at a zenith distance of 50° , one taken with the ADC tracking and the other with it nulled. In this example, about 65 per cent of the UV light and 50 per cent of the near-infrared flux missed the 2 arcsec diameter fibre when the ADC was nulled. See text for details.

short-exposure (5 s) spectra of a bright hot star, observed in good seeing (0.9 arcsec) at a zenith distance of 50° ; a spectrum taken with the ADC nulled has been divided by an otherwise identical spectrum taken with the ADC tracking. The star was the ninth-magnitude Wolf–Rayet star HD 76536, which has broad emission lines up to 10 times stronger than the continuum. The virtually perfect cancellation of these dominant features demonstrates that the spectra have been well calibrated in wavelength. In this case, the spectrum taken without the ADC misses up to 65 per cent of the UV flux and 50 per cent of the infrared flux. The numerical losses depend strongly on the effective wavelength at which the uncorrected image is acquired, the seeing and any positioning errors, as well as the zenith distance.

5.3 Positioner

The accuracy, speed and reliability of the positioner are all crucial for efficient operation of 2dF.

The positioner internal precision is set to $20\ \mu\text{m}$ (0.3 arcsec) by requiring that the robot keep repeating the placement of each button until the actual position is within $20\ \mu\text{m}$ of the demanded

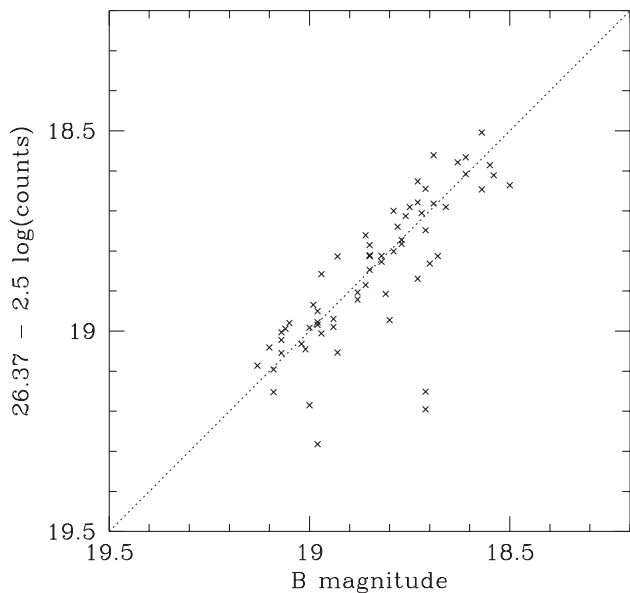


Figure 13. Counts versus magnitude plot for a sample of 67 main-sequence stars in the globular cluster Omega Centauri, from a total exposure of 10 hours per star in the blue spectral range. The zero-point of the ordinate has been chosen to give the best fit to a 45° line after discarding three discrepant points. The remaining stars show an rms scatter of 0.07 mag or about 7 per cent in flux; the component of this scatter arising from positioning errors is at most 5 per cent.

position (Section 3.6); normally the average number of iterations per fibre move is much less than unity. The external accuracy actually achieved is much harder to assess since it depends on many factors: the reliability of the input target positions (which in turn can involve several effects such as proper motions, magnitude or colour-dependent astrometric errors, and inaccurate transformations from some original x, y coordinate system to RA and Dec.); the accuracy with which the 2dF gantry system has been calibrated (Section 4.1); and the stability of the robot during the hour or so required to do a full configuration, which itself may be a function of the zenith angle of the telescope (since configuring is usually done while observing the previous field).

The overall positioning accuracy of 2dF can be assessed in three ways: by how well the four guide stars can be acquired simultaneously; by comparing the counts in each fibre with the known magnitudes of the target objects; and by taking offset exposures to determine the actual positions of targets relative to the fibres. The first two ways are used routinely during normal observations and can quickly show if there is a problem; the last is a time-consuming procedure used only for tests of the system. If the guide star positions appear to be inconsistent, a simple check can be done by asking the FPI imaging CCD to determine the centroid for each star.

The best tests of the system are observations of moderately bright ($V \sim 15$) stars in Galactic clusters or the Magellanic Clouds; such samples of stars are often restricted to narrow ranges of magnitude and colour, and all have virtually identical proper motions. Sometimes the guide stars can be selected from the same target sample. In the best cases, all four guide stars will be well centred simultaneously and the plots of counts versus magnitude (available routinely within the 2DFDR reduction software) will show a scatter of no more than ± 0.2 mag, implying that all fibres have been correctly placed to better than 0.5 arcsec. An example of this is shown in Fig. 13. The fact that such good results are

obtainable indicates that the inherent accuracy of the 2dF robot is at that level, and that most of the worse results must be a consequence of either bad input data or a poorly calibrated positioner. In general, the counts versus magnitude plots have larger scatter, particularly for targets near the edge of the field, and there are often a few outliers with very low counts, corresponding to position errors larger than the 1-arcsec radius of the fibres. Of course the counts versus magnitude plots show much greater scatter for extended galaxies, since a variable fraction of the total galaxy light enters the fibre, and the astrometric tolerances for such targets can be somewhat looser. Work is continuing on the precise calibration of the positioner, and on determining the best values of parameters such as the temperature dependence of the plate scales.

The speed of the positioner is approximately 6 s per fibre move, so that a full re-configuration of all 400 fibres (requiring ~ 600 moves) takes about 1 hour. The original 2dF specification was to take only 30–40 min per reconfiguration, but since an elapsed time of close to an hour was found to be optimal for the redshift surveys (allowing for the necessary calibration exposures and CCD readouts) this was relaxed somewhat. The original specification was driven by the need to re-configure fields to counter the effects of atmospheric refraction, but this has turned out rarely to be an operational constraint since the limiting time would only be an hour at rather extreme zenith distances. Observing at large zenith distances is discouraged in any case, since the positioner accuracy and reliability deteriorate.

The reliability of the positioner was originally specified to be no worse than $1:10^5$ per fibre move, on the grounds that a failure was liable to be catastrophic and could lead to the loss of hours of observing time if there was a major fibre tangle or many breakages. Such serious failures must not occur more than once per lunation. Initially, when 2dF observations began, the failure rate was much worse than this. However, the incidence of catastrophic failures has become very low as various improvements have been made to the hardware and control software. The current rate of positioner failures of all types averages approximately $1:10^4$ fibre movements, but most failures are relatively trivial, cause no serious damage and cost only minutes to fix.

5.4 Optical fibres

The variations in fibre throughput are small. The overall scatter, as measured from the throughput calibrations determined by 2DFDR, is less than 20 per cent for most of the fibres and this includes the variations of 15 per cent in fibre cross-section from field centre to edge, plus any variations in the prisms at the input ends. A few fibres have lower transmission by factors of about 2, presumably because of misaligned prisms, dirt or other accidents (parked fibres appear to have systematically lower transmission, less than half the normal value, but this is simply due to vignetting). The throughputs appear to be stable with time. There is little evidence for differences in fibre transmission with wavelength: any such variations are essentially trivial, compared with the differences in spectral shape introduced by the radial variations (CVD) intrinsic to the 2dF optics (see Section 3.2) combined with fibre positioning errors.

Occasionally, spectra appear with a marked saw-tooth intensity variation of amplitude up to 20 per cent; the number of oscillations can range from two or three to a dozen or more, with the period of the variations increasing linearly with actual wavelength. These appear to be an effect of interference fringing, probably arising from cracks in the fibres or some fault at their terminations. The

Table 2. Properties of pairs of gratings available for use with 2dF.

Grating	ρ	λ_b	dispersion (nm pixel ⁻¹)	resolution (nm)
300B	300	420	0.43	0.90
270R ¹	270	760	0.48	1.0
316R ¹	316	750	0.41	0.85
600V	600	500	0.22	0.44
1200B	1200	430	0.11	0.22
1200V	1200	500	0.11	0.22
1200R	1200	750	0.11	0.22

λ_b is the Littrow blaze wavelength. The resolution is the effective instrumental resolution, either the projection of the fibre on to the detector or 2 pixels, whichever is the larger. ρ is the ruling density (line mm⁻¹).

¹The 270R grating is paired with a 316R grating since the 270R grating master was no longer available when a duplicate was ordered.

variations are usually removed or much reduced by the standard flat-fielding procedure in 2DFDR but this sometimes fails, either because the fibres are unstable or through some error in the flat-fielding process.

5.5 Spectrographs

The optical quality of the spectrographs is such that each fibre image is focused to a resolution of about 2 pixels. Typical values of arc linewidths are a FWHM of 2.1 pixels for spectrograph No. 1 and 1.9 pixels for spectrograph No. 2. These values yield resolutions with the various gratings as shown in Table 2. There is some variation in spectral resolution across the CCDs, owing to a deterioration of image quality in the corners of the field; this affects in particular the spectral resolution at the UV and near-infrared ends of spectra in the first and last slit blocks (spectrum numbers 1–10 and 191–200). This variation in point spread function across the field sets one limit to the accuracy of sky subtraction; even if the intensities are calculated correctly, the changes in line profile lead to residual P Cygni-type dips and spikes at the locations of strong night sky emission lines. The change in image quality also leads to poorer spatial resolution, and hence to occasional problems with fitting the tramline map which is used to extract the 1D spectra.

The optical imaging quality of the spectrographs does limit their usefulness in some ways. There is significant astigmatism at high grating angles, making it impossible to use them effectively in second order and degrading their performance with the 1200 line mm⁻¹ gratings at the near-infrared end of the wavelength range (e.g. for the Ca II triplet near 8600 Å). It is possible to set good focus in either the spatial or the spectral direction, but not both simultaneously.

The focus of the spectrographs is quite strongly dependent on temperature, sometimes necessitating re-focusing during the course of the night if the ambient temperature changes by more than a few degrees.

Flexure in the spectrographs is at the level of ~ 0.2 pixels per hour. For most observing programmes, individual exposures are for at most 30 or 40 min in order to control cosmic ray contamination, and it is standard practice to take calibration arc exposures every hour or so. For the main redshift surveys, which are done at low resolution with the 300B gratings, the accuracy of velocity determinations for galaxies (determined from repeat observations of the same targets) is about 65 km s⁻¹ for the best quality data and around 100 km s⁻¹ on average (Colless et al. 2001). Much higher accuracies are attainable for stars observed at high resolution with

the 1200 line mm⁻¹ gratings: typical values are in the range 5–10 km s⁻¹.

The throughput of the spectrographs is reasonably uniform across the full field of view, with a scatter of about 10 per cent with no drop-off towards the edges of the CCD, much superior to the earlier AUTOFIB system when used with the RGO Cassegrain spectrograph. Scattered light is, however, a significant problem which manifests itself in various ways. Direct measurement of scattered light can be done in the spectral direction by looking at the profiles of isolated strong arc lines, or in the spatial direction by illuminating a single fibre. Alternatively, the total scattered light in a data frame can be estimated from the residual signal in broken or masked-off fibres. All these methods give consistent results. The total amount of light scattered from a single illuminated pixel to other pixels on the CCD is between 10 and 20 per cent of the input signal; the exact amount varies with wavelength and location in the field. Another measure is that about 1 per cent of the light in a single fibre is scattered into each of the immediately adjacent fibre locations on the CCD (note that this virtually all occurs within the spectrograph; there is no detectable ‘cross-talk’ between fibres before they reach the spectrographs). A practical consequence of this is that it is inadvisable to try to observe stars with too wide a range in magnitude simultaneously, and it is important to avoid accidentally hitting any bright stars when observing faint targets.

Correction for any scattered light is important for the proper determination of relative fibre throughputs and for accurate sky subtraction. It is also of course essential for the measurement of the equivalent widths of absorption features. For fields of relatively faint targets, or whenever the range of signal strengths in different fibres is small, the total scattered light distribution can be approximated by a smoothly varying function across the CCD. This is the approach used in the redshift surveys and is the default option within 2DFDR; a mean background map is determined by fitting to the signal in broken fibres and at the edge of the frame, and this is then subtracted from the data (Bailey et al. 2002). The accuracy of sky subtraction in the redshift surveys is typically 2–5 per cent, although much worse values are sometimes reported.

A special type of scattered light arises in the case of halation, which is sometimes a serious problem especially in spectrograph camera No. 2. A condensate slowly builds up on the field flattener lens in front of the CCD and causes the formation of haloes around bright sources. These usually appear as shoulders or a pedestal at the base of strong emission lines, or adjacent to bright stars in the spatial direction. In some early 2dF data this halation could contribute a further 10–15 per cent to the total scattered light. This then substantially degraded the data, since it gave rise to both a loss of signal (the total amount lost to scattering must be considerably larger than the numbers reported here, which refer only to the light that lands on the CCD) and an increase in noise. However, it can be kept to much lower limits by careful monitoring and regular pumping of the cryogenic CCD cameras.

The level of light leaking from the fibre back-illumination within the spectrograph is a potential cause for concern. This can be tested by illuminating the fibres continuously while taking a dark CCD exposure and measuring the excess signal over a similar length exposure with no fibre back-illumination. This has to be repeated for both spectrographs and both plate combinations. Typically < 1 ADU of additional diffuse background signal is measured from the permanently back-illuminated case in a 5-min dark exposure. In normal use the back-illumination is only switched on when the positioner robot requires to see the fibre. This results in a duty cycle of less than 10 per cent so the light leaking from the

back-illumination is insignificant for the typical length exposures of 20–40 min. True dark current in the 2dF CCDs is at a negligible level for most purposes.

The quality and stability of the CCDs and controllers are very good and there is normally no need to take bias frames. The bias counts are well subtracted by using data from the overscan region of the data frames.

Details of the characteristics and performance of the CCDs can be obtained from the 2dF WWW pages (<http://www.aao.gov.au/2df/>). The two Tek 1024 CCDs in use in 2dF are very similar in all respects. Prior to 1999 September an engineering-grade CCD was in use in spectrograph camera No. 2; this too had similar characteristics, but with a few bad columns and some other cosmetic defects.

5.6 Data reduction and calibration

The pipeline data reduction system 2DFDR is a crucial component of 2dF, enabling observers to assess data quickly during the night and to come away at the end of an observing run with fully reduced data. This was essential for the redshift surveys, where it was necessary to keep pace with the incoming data and the quasi-online data reductions had to be the final output. For most other projects, the many options within 2DFDR make it a very powerful and convenient tool for producing high-quality reduced data, provided that it is used carefully and with a full understanding of the procedures.

Aspects of the performance of 2DFDR are discussed in the 2dF User Guide (<http://www.aao.gov.au/2df/>), by Bailey et al. (2002), by Colless et al. (2001) in the context of the redshift survey and in preceding sections of this paper.

There remain some situations where it is not initially clear whether a particular problem is a feature of the 2dF instrument itself or an artefact of the data reduction process. A good example was afforded by the demonstration by Croom et al. (2001) that there are apparent systematic variations in throughput across the 2dF field. Their fig. 5 is a contour plot, showing the difference between the actual counts obtained and the expected magnitudes for over 20 000 quasar candidates in the 2dF Quasar Redshift Survey. It appears that the 2dF throughput is systematically low at the western edge of the field, and that the peak throughput is offset towards the eastern edge, well away from the field centre; the amplitude of the effect is ± 0.4 mag or about a factor of 2. This result led to a rapid checking of the astrometric and imaging performance of 2dF, but it seemed that neither positioning errors nor variations in focus or image structure could explain the effect. A similar effect, but at somewhat lower amplitude, was seen in the corresponding Galaxy Redshift Survey data.

It transpired that the cause lay in a partial failure of the sky subtraction procedure, combined with some details of the way in which the software calibrates the relative fibre throughputs. Spectra near the edges of the CCD frame in the 2dF spectrographs have slightly poorer resolution than the majority; this led to an underestimate of the strength of night sky lines in the spectra and an over-correction of the fibre throughput. Both effects led to an artificial increase in the photon counts for spectra near the edges of the CCDs, which happen to come from fibres that populate the eastern part of the 2dF field; conversely, spectra near the centre of the CCD which correspond to the western part of the field (and which are actually the best quality spectra) appeared to be giving fewer counts. Correction of the original sky subtraction error led to a much more symmetrical plot of counts versus magnitude, in

Table 3. Broad-band total efficiency measurements.

Passband and magnitude	wavelength (nm)	electrons $\text{s}^{-1}\text{\AA}^{-1}$	efficiency (per cent)
$B = 17$	440	0.6	2.8
$V = 17$	550	0.6	4.3
$R = 17$	700	0.4	4.7

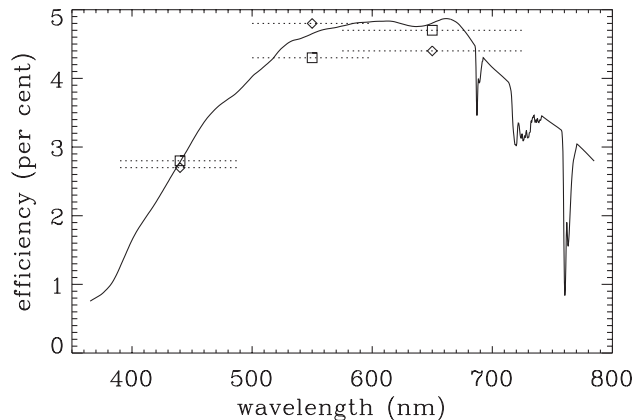


Figure 14. The total 2dF system efficiency with 300B gratings as a function of wavelength. The squares and diamonds represent broad-band absolute efficiency measurements from 1997 January and 1999 November, respectively. The solid line was obtained from a relative throughput calibration using data from 2001 January scaled to match the broad-band measurements approximately.

which the peak is at the field centre and there is some decrease all round the periphery, as expected given the larger astrometric errors and somewhat worse imaging towards the edge of the 2dF field.

5.7 System throughput

The total system throughput (including atmosphere, telescope, fibres, instrumentation and detector quantum efficiency) has been determined by observing fields of several dozen photometric standard stars to allow an average to be determined over a large number of fibres. With the 300B grating we measured the absolute efficiency (corrected to 1.0-arcsec seeing) with typical values as given in Table 3.

Since the wavelength information in these broad-band measurements was insufficient, an improved relative throughput calibration was derived using about 100 stars observed simultaneously with 2dF (Fig. 14). The relative efficiency versus wavelength was determined by dividing the observed spectra by model spectra that were chosen to match best the broad-band magnitudes of the stars.

Of course these efficiencies change with choice of grating; the best performance comes with the use of the low-resolution 270R and 316R gratings where the blaze of the grating matches the peak of the CCD quantum efficiency. In this case the system efficiency peaks at 9 per cent. For more details and signal-to-noise ratio calculations, see the 2dF WWW pages (<http://www.aao.gov.au/cgi-bin/2dfsn.cgi>).

5.8 Special sky subtraction techniques

While the main effort has gone into optimizing the use of 2dF for the large redshift surveys, i.e. for very large numbers of

low-dispersion observations of relatively bright targets, it is clear that 2dF can be used in many other ways. Some of the scientific programmes are described in the following section. Here we mention some technical factors relevant to other applications of 2dF.

The biggest questions are how faint can 2dF observations be pushed, and what is the best way of maximizing the signal-to-noise ratio in a given observing time? This comes down to two further questions: what is the best way of doing sky subtraction, and for how long can observations be continued and still give a useful gain?

The redshift survey data, on which many of the performance figures quoted above are based, typically consist of sets of 3×1100 -s integrations on sets of galaxies to $B \sim 19.5$. The mean dark sky signal is approximately equal to 20 per cent or less of the signal for most galaxies. For such observations, the standard procedure is to allocate a fraction (at least 5 per cent) of the fibres to random sky positions, derive a mean sky and scale this for each fibre. The same technique will work for total integration times of several hours and should produce similar quality data for targets up to 1 or 2 mag fainter. Beyond that, the observations will be sky-limited and the gains will go as the square root of the observing time, at best.

Two alternative techniques are classical beam switching, in which pairs of fibres are placed equal distances apart and each target is observed alternately in either fibre, and ‘nod & shuffle’ (Glazebrook et al. 1999; Glazebrook & Bland-Hawthorn 2001), where the image is moved rapidly (‘shuffled’) between an active and a storage area on the CCD, exactly in phase with the nodding of the telescope between targets and an offset sky position. Experiments with both methods were done with 2dF in 2001 January. In theory, the ‘nod & shuffle’ method should give the best results since an identical optical path is used for the target and sky observations, and because the switching is very fast compared with the time-scale of night sky line variations. Beam switching should be almost as good when time variations are not critical and has the advantage that the target is always being observed, whereas ‘nod & shuffle’ is off-source for half the time. Both types of switching are inefficient compared with conventional observing, in terms of the number of targets observable.

In practice neither mode gave dramatic gains in the magnitude range accessible to 2dF, although sky subtraction can be improved to below 1 per cent using these methods. A serious drawback of any target–sky switching technique is that it depends on finding clean sky apertures at the same fixed distance from every target. This becomes harder as the number of targets increases. Moreover, to avoid damaging the signal for an object at, say, magnitude 21, it is necessary to have no objects in the sky aperture that are brighter than magnitude 24 or 25, well below the detection limit of the Schmidt sky surveys or most wide-field CCD images.

Essentially, the preferred method of sky subtraction depends on whether the limit is set by photon statistics and faint object contamination in the sky, or by the systematic errors involved in transferring the sky from other fibres. In the case of 2dF, it seems that the operational complications and target losses inherent in beam switching mean that it is usually better to try to minimize the systematic errors and to continue to use the mean sky approach.

A more fruitful line may be to exploit the large numbers of objects observable with 2dF to create mean spectra, rather than trying to increase the signal-to-noise ratio in each individual spectrum. One approach is to take large numbers of targets selected to be almost identical from other evidence (e.g. photometry, or an automatic spectral classification scheme) and combine their

spectra; a second is to subdivide samples according to one or more strong spectroscopic features, and then to combine the subsets to look for weaker features which may correlate with the strong features. Either way, spectra can be created with signal-to-noise ratio levels corresponding to hundreds or even thousands of hours of observation.

5.9 Configuration efficiency

The current version of the CONFIGURE software, which allocates fibres to targets, has been optimized for the Galaxy Redshift Survey (Colless et al. 2001). This is characterized by having a mean target density of about 180 per square degree, fairly uniformly distributed across the sky, so that it was necessary to have an algorithm that could achieve a very high yield in allocating all 400 fibres when there were often only about 400 targets in the 2dF field. The Galaxy Redshift Survey is able to allocate fibres to 94 per cent of the original input target list (Colless et al. 2001).

Somewhat different constraints arise in other applications, e.g. in crowded globular star clusters, in deep fields from CCD images, or when there are many fewer than 400 targets. CONFIGURE has several options for different ways of allocating fibres to targets, and these can sometimes give substantially higher yields than running the default parameters. For example, in crowded compact fields, it is best to centre the targets and to limit the pivot angle through which fibres can move. However, the maximum yields in very compact fields are not high, owing to the size and shape of the 2dF buttons and the requirement to leave safe clearance between buttons and fibres. Over 300 fibres can be allocated to targets within a 1° diameter field, and approximately 100 fibres can be allocated to objects in a 20 arcmin diameter field, based on observations of dense globular clusters.

For sparse fields with fewer than 200 targets, it is often more efficient to restrict the fibres to a single spectrograph, if only for ease of data reduction. For covering a wide range of magnitudes, e.g. in Galactic open star clusters, the targets should be split into subsets covering only 2 or 3 mag each. Note that the reconfiguration time becomes very short for small samples of stars, so it is not inefficient to use 2dF for observations of relatively small numbers of bright stars (50 stars take about 5 min to configure).

Other techniques have also been used with the CONFIGURE software to send the light from blue objects to one spectrograph with a blue grating and red objects to the second spectrograph with a red optimized grating. A good example of this is given by Glazebrook et al. (2001).

2dF is not very efficient for doing short observations of single targets such as standard stars. There is a procedure for placing a star down any desired fibre in an existing configuration, but it is rather slow and cumbersome, and it depends on blind offsetting from a guide fibre to a target fibre. If it is desired to measure many such stars, a better procedure is to prepare a special configuration with just a few fibres in a simple pattern at the field centre. For long observations of single targets where accurate centring is important, it is necessary to have one or more bright guide stars in the same way as for a full 2dF configuration. This applies especially to faint ‘targets of opportunity’ where it is essential to supply a target position, sky positions and a nearby guide star.

A key design feature of 2dF, which has been little exploited up to now, is the ability to keep track of differential atmospheric refraction by setting up the same configuration on both field plates, but corrected for different hour angles. To observe the same field all night one should tumble between the two plates every hour or

two, depending on telescope attitude (see Fig. 1). However, setting up such configurations is not trivial because there are small but significant geometrical differences between the two 2dF fieldplates. These mean that a configuration that is valid on one plate will fail on the other because of button and fibre collisions,

and because limits on fibre extensions and pivot angles are exceeded. These effects can be largely avoided by setting up the starting configuration with extra clearance around the buttons and reduced limits on the pivot angle. The minimum clearance, set by the 2dF hardware, is 400 μm ; setting this to 800 μm and setting the

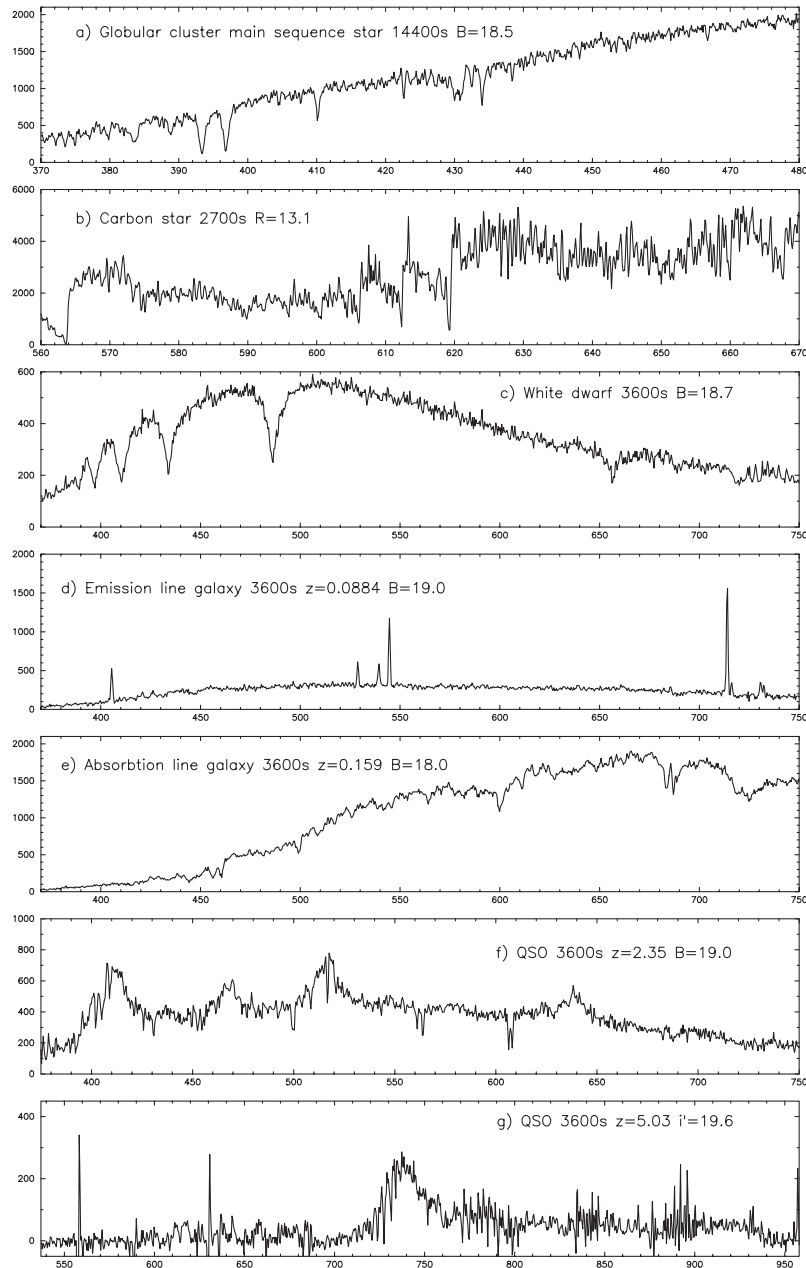


Figure 15. Some examples of spectra taken with 2dF. The first two are high-dispersion stellar spectra (1200 line mm^{-1} gratings, $2\text{-}\text{\AA}$ resolution); the next four are low-dispersion spectra covering almost the full wavelength range accessible to 2dF, taken with the 300B gratings for the galaxy or quasar surveys. The final panel shows a low-dispersion spectrum taken with the 316R grating. The exposure times and magnitudes are quoted in each panel. The X-axis of each panel is the wavelength in nm; the Y-axis is the observed number of counts after data reduction. (a) Blue spectrum of a faint main-sequence star in the globular cluster 47 Tucanae, in which the dominant features are the H & K lines of Ca II near 390 nm, the CH G-band near 430 nm and several Balmer H lines. (b) Red spectrum of a carbon star in the SMC, showing the deep Swan C₂ band near 560 nm and several strong spikes between 605 and 620 nm due to the combined effects of C₂ and CN bands (the noisy appearance of this quite high signal-to-noise ratio spectrum is due to a host of real molecular features: such spectra yield radial velocities with an internal precision of 3 km s^{-1}). (c) A foreground white dwarf star typical of many found in the colour-selected 2QZ quasar survey, with broad Balmer H absorption lines. (d) A strong emission-line galaxy from the 2dF Galaxy Redshift Survey, with lines due to redshifted [O II] near 407 nm, H β and [O III] near 540 nm, and H α near 710 nm. (e) An absorption-line galaxy with lines due to redshifted H & K Ca II absorption near 460 nm, Mg b absorption at 600 nm, and Na D near 685 nm (next to the atmospheric B-band O₂ absorption feature). (f) A QSO from the 2QZ survey with broad emission lines of Ly α near 410 nm, Si IV near 470 nm, C IV near 520 nm and C III] near 640 nm. (g) A QSO identified as part of a joint 2dF–SDSS observing programme (Glazebrook et al. 2001) with broad Ly α near 730 nm. With thanks to S. Croom (private communication) for the spectra shown in panels (c) and (f).

maximum pivot angle to 10° instead of the default 14° largely avoids collisions when switching fieldplates or changing the configuration hour angle. There may be a decreased target yield since the fibres cannot be placed so close together, but in practice such losses are generally only a few per cent.

6 2dF SCIENCE

While the main science driver for the design of 2dF has been the large redshift surveys (Colless et al. 2001; Croom et al. 2001), the inherent flexibility in the design of 2dF means that it is a unique facility for many other types of astronomy.

A diverse range of both galactic and extragalactic astronomy problems have already been tackled using the unique area coverage and multiplex advantage of 2dF. Some of these are described briefly in this section. Some examples of spectra obtained with 2dF are shown in Fig. 15.

Gilmore, Wyse, Norris and Freeman are using 2dF to measure radial velocities to an accuracy of 10 km s^{-1} for several thousand F/G main-sequence stars at distances of 3–7 kpc from the Sun in several sightlines through the Galaxy (Gilmore & Wyse 2001). These data will allow the statistical study of the kinematics and metallicity distributions of stars in the Galactic thick disc and halo. Initial results include a new population of low-metallicity stars with disc-like kinematics, possibly representing debris from a merged satellite.

Spectroscopy of large samples of faint stars in globular clusters have been obtained by Cannon, Croke, Da Costa and Norris (private communication). Their objective is to compare the chemical abundance variations seen in red giant stars with unevolved main-sequence stars to determine whether these variations are due to self-enrichment during evolution or are primordial. In the case of 47 Tucanae, the spectra show clear separation into CN-strong and CN-weak stars. Combining the spectra for 50–100 stars in each class yields very high signal-to-noise ratio spectra with more than 10^5 counts per pixel, making it possible to detect extremely weak features and to look for correlations with other abundance parameters.

Hatzidimitriou et al. (2000) have been using 2dF to study carbon stars in the Magellanic Clouds. Two observing runs yielded over 2000 carbon star spectra in both Clouds. These spectra have been used to map in fine detail the rotation and velocity dispersion across the Large Magellanic Cloud (LMC). The data are also being used to classify and determine chemical abundances for the carbon stars.

Evans and Howarth (private communication) are using 2dF to undertake a spectroscopic survey of massive stars in the Small Magellanic Cloud (SMC) from an unbiased sample of bright blue field stars obtained from APM photometry. Over 4000 intermediate-resolution spectra have already been obtained and used to generate an observational Hertzsprung–Russell diagram. This can be compared with population synthesis models to investigate the field star initial mass function for the SMC.

Drinkwater et al. (2000) are carrying out a complete, unbiased survey of the Fornax cluster by obtaining 2dF spectra for all objects down to $b_J = 19.7$ in a 12 square degree region centred on the cluster. The goals of this project are to determine cluster membership for a complete sample of objects (especially dwarf galaxies), to study the cluster dynamics, to detect previously unrecognized compact galaxies in the cluster and field, and to study background galaxies and quasars and foreground Galactic stars.

A deep narrow-band [O III] imaging survey of the Virgo cluster

has revealed a large population of emission-line objects that could be either planetary nebulae associated with the intracluster medium or high-redshift emission-line galaxies. During a 5-h 2dF exposure, Freeman et al. (2000) obtained 47 emission-line detections, of which 23 turned out to be true intracluster planetary nebulae with detection of both the 4959- and 5007-Å lines, and another 16 in the outer regions of M87. Freeman et al. also found eight Ly α emitters at $z \sim 3.1$ with equivalent widths $W_\lambda(\text{Ly}\alpha) > 150 \text{ \AA}$.

Willis, Hewett & Warren (2001) have compiled a sample of 485 early-type galaxies with redshifts with $0.3 \leq z \leq 0.6$. This represents the largest sample of luminous field galaxies at intermediate redshift. These data are being used to study the evolution of galaxy clustering on large scales, for an investigation of the Fundamental Plane for luminous galaxies as a function of environment, and for a survey for strong gravitational lensing.

7 FUTURE PLANS

In this paper we have described a unique multi-object optical spectroscopy facility (2dF) available as a common-user instrument at the Anglo-Australian Telescope.

We are currently performing experiments using 2dF with techniques such as charge shuffling and telescope nodding (Glazebrook & Bland-Hawthorn 2001) to improve the sky subtraction of extremely faint target objects.

Future plans include replacing the two spectrographs with bench-mounted spectrographs using volume phase holographic (VPH) grating (Barden, Arns & Colburn 1998) technology. The VPH gratings have the advantage of offering higher efficiency than conventional reflecting diffraction gratings. Upgraded detectors, improved anti-reflection coatings and new optical fibre materials (Shöltz et al. 1998) will allow us to use longer optical fibres and still gain in overall throughput and provide higher resolutions. The advantage of the bench-mounted spectrographs will be in their thermal and mechanical stability.

We also plan to use the flexibility of the fieldplate tumbler system to provide one or two fibre feeds for integral field spectroscopy at the currently unused 90° positions of the 2dF tumbler unit.

ACKNOWLEDGMENTS

The authors acknowledge the many AAO technical staff who have made 2dF a reality, and astronomy support staff of the AAO who make 2dF available to the general user. This project has only been possible with extensive support from both the Australian and UK scientific communities and the long-term backing of the AAT Board.

REFERENCES

- Bailey J. A., Glazebrook K., Offer A. R., Taylor K., 2002, MNRAS, submitted
- Barden S. C., Armandroff T., Muller G., Rudeen A. C., Lewis J., Groves L., 1994, in Crawford D. L., Craine E. L., eds, Proc. SPIE 2198, Instrumentation in Astronomy VIII. SPIE, Bellingham, p. 87
- Barden S. C., Arns J. A., Colburn W. S., 1998, in D’Odorico S., ed., Proc. SPIE 3355, Optical Astronomical Instrumentation. SPIE, Bellingham, p. 866
- Cannon R. D., 1997, in Kontizas E., Kontizas M., Morgan D. H., Vettolani G. P., eds., Wide-Field Spectroscopy. Kluwer, Dordrecht, p. 33
- Cannon R. D., 2000, AAO Newsletter, 92, 14
- Colless M. et al., 2001, MNRAS, 328 1039

- Croom S. M., Smith R. J., Boyle B. J., Shanks T., Loaring N., Miller L., Lewis I. J., 2001, *MNRAS*, 322, L29
- Drinkwater M. et al., 2000, *A&A*, 355, 900
- Farrell T. J., Bailey J. A., Shorridge K., 1995, in Shaw R. A., Hayes J. J. E., eds, *ASP Conf. Ser. Vol. 77, Astronomical Data Analysis and Systems IV*. Astron. Soc. Pac., San Francisco, p. 133
- Freeman K. C. et al., 2000, in Combes F., Mamon G. A., Charmandaris V., eds, *ASP Conf. Ser. Vol. 197, 15th AIP Meeting, Dynamics of Galaxies*. Astron. Soc. Pac., San Francisco, p. 389
- Gilmore G., Wyse R. F. G., 2001, in Deiters S., Fuchs B., Just A., Spuzem R., Wielen R., eds, *ASP Conf. Ser. Vol. 228, Dynamics of Star Clusters and the Milky Way*. Astron. Soc. Pac., San Francisco, p. 225
- Glazebrook K., Bland-Hawthorn J., 2001, *PASP*, 113, 197
- Glazebrook K., Bland-Hawthorn J., Farrell T. J., Waller L. G., Barton J. R., Lewis I. J., 1999, *AAO Newsletter*, 90, 11
- Glazebrook K., Tsvetanov Z., Zheng W., Hoversten E., Chiu K., Bridges T., Boyle B., 2001, *AAO Newsletter*, 98, 4
- Gray P. M., 1983, in Bokserberg A., Crawford D. L., eds, *Proc. SPIE 445, Instrumentation in Astronomy V*. SPIE, Bellingham, p. 57
- Gray P. M., Taylor K., 1990, in Crawford D. L., ed., *Proc. SPIE 1235, Instrumentation in Astronomy VII*. SPIE, Bellingham, p. 709
- Gray P. M., Taylor K., Parry I. R., Lewis I. J., Sharples R. M., 1993, in Gray P. M., ed., *ASP Conf. Ser. Vol. 37, Fibre Optics in Astronomy II*. Astron. Soc. Pac., San Francisco, p. 145
- Guerin J., Bellenger R., Dreux M., Felenbok P., Fernandez A., Rousset G., Schmidt R., 1993, in Gray P. M., ed., *ASP Conf. Ser. Vol. 37, Fibre Optics in Astronomy II*. Astron. Soc. Pac., San Francisco, p. 138
- Hatzidimitriou D., Cannon R. D., Croke B. F., Morgan D. H., 2000, in Combes F., Mamon G. A., Charmandaris V., eds, *ASP Conf. Ser. Vol. 197, 15th AIP Meeting, Dynamics of Galaxies*. Astron. Soc. Pac., San Francisco, p. 347
- Hill J. M., Lesser M. P., 1986, in Crawford D. L., ed., *Proc. SPIE 627, Instrumentation in Astronomy VI*. SPIE, Bellingham, p. 303
- Høg E. et al., 2000, *A&A*, 357, 367
- Jenkins C. R., Gellatly D. W., Bingham R. G., Worswick S. P., 1993, in Gray P. M., ed., *ASP Conf. Ser. Vol. 37, Fibre Optics in Astronomy II*. Astron. Soc. Pac., San Francisco, p. 209
- Jones D. J. A., 1993, in Gray P. M., ed., *ASP Conf. Ser. Vol. 37, Fibre Optics in Astronomy II*. Astron. Soc. Pac., San Francisco, p. 355
- Jones D. J. A., 1994, *Appl. Opt.*, 33, 7362
- Lewis I. J., Parry I. R., 1990, in Crawford D. L., ed., *Proc. SPIE 1235, Instrumentation in Astronomy VII*. SPIE, Bellingham, p. 745
- Lewis I. J., Parry I. R., Sharples R. M., Taylor K., 1993, in Gray P. M., ed., *ASP Conf. Ser. Vol. 37, Fibre Optics in Astronomy II*. Astron. Soc. Pac., San Francisco, p. 249
- Lewis I. J., Glazebrook K., Taylor K., 1998a, in Arribas S., Mediavilla E., Watson F. G., eds, *ASP Conf. Ser. Vol. 152, Fibre optics in Astronomy III*. Astron. Soc. Pac., San Francisco, p. 71
- Lewis I. J., Glazebrook K., Taylor K., 1998b, in D'Odorico S., ed., *Proc. SPIE 3355, Optical Astronomical Instrumentation*. SPIE, Bellingham, p. 828
- Parker Q. A., Watson F. G., Miziarski S., 1998, in Arribas S., Mediavilla E., Watson F. G., eds, *ASP Conf. Ser. Vol. 152, Fibre optics in Astronomy III*. Astron. Soc. Pac., San Francisco, p. 80
- Parry I. R., Gray P. M., 1986, in Crawford D. L., ed., *Proc. SPIE 627, Instrumentation in Astronomy VI*. SPIE, Bellingham, p. 118
- Parry I. R., Sharples R. M., Lewis I. J., Gray P. M., 1993, in Gray P. M., ed., *ASP Conf. Ser. Vol. 37, Fibre Optics in Astronomy II*. Astron. Soc. Pac., San Francisco, p. 36
- Parry I. R., Lewis I. J., Sharples R. M., Dodsworth G. N., Webster J., Gellatly D. W., Jones L. R., Watson F. G., 1994, in Crawford D. L., Craine E. L., eds, *Proc. SPIE 2198, Instrumentation in Astronomy VIII*. SPIE, Bellingham, p. 125
- Roeser S., Bastian U., 1988, *A&AS*, 74, 449
- Royal Astronomical Society Report, 1986, Review of Scientific Priorities for UK Astronomical Research 1990 to 2000. RAS, London
- Sadler E. M., Harrison S., Lee S., 1991, *AAO Observing Guide UM1.4*
- Shectman S. A., 1993, in Gray P. M., ed., *ASP Conf. Ser. Vol. 37, Fibre Optics in Astronomy II*. Astron. Soc. Pac., San Francisco, p. 26
- Shöltz G. F., Vydra J., Lu G., Fabricant D., 1998, in Arribas S., Mediavilla E., Watson F. G., eds, *ASP Conf. Ser. Vol. 152, Fibre optics in Astronomy III*. Astron. Soc. Pac., San Francisco, p. 20
- Smith G., Lankshear A., 1998, in D'Odorico S., ed., *Proc. SPIE 3355, Optical Astronomical Instrumentation*. SPIE, Bellingham, p. 905
- Taylor K., Gray P. M., 1990, in Barr L. D., ed., *Proc SPIE 1236, Advanced Technology Optical Telescopes IV*. SPIE, Bellingham, p. 290
- Taylor K., Gray P. M., 1993, in Gray P. M., ed., *ASP Conf. Ser. Vol. 37, Fibre Optics in Astronomy II*. Astron. Soc. Pac., San Francisco, p. 379
- Taylor K., Gray P. M., 1994, in Crawford D. L., Craine E. L., eds, *Proc. SPIE 2198, Instrumentation in Astronomy VIII*. SPIE, Bellingham, p. 136
- Taylor K., Bailey J. A., Wilkins T., Glazebrook K., 1996a, in Jacoby G. H., Barnes J., eds, *ASP Conf. Ser. Vol. 101, Astronomical Data Analysis and Systems V*. Astron. Soc. Pac., San Francisco, p. 195
- Taylor K., Cannon R. D., Watson F. G., 1996b, in Ardeberg A., ed., *Proc SPIE 2871, Optical Telescopes of Today and Tomorrow*. SPIE, Bellingham, p. 145
- Watson F. G., Gray P. M., Oates A. P., Lankshear A., Dean R. G., 1993, in Gray P. M., ed., *ASP Conf. Ser. Vol. 37, Fibre Optics in Astronomy II*. Astron. Soc. Pac., San Francisco, p. 171
- Wilcox J. K., 1993, in Gray P. M., ed., *ASP Conf. Ser. Vol. 37, Fibre Optics in Astronomy II*. Astron. Soc. Pac., San Francisco, p. 51
- Willis J. P., Hewett P. C., Warren S. J., 2001, *MNRAS*, 325, 1002
- Wynne C. G., 1989, *MNRAS*, 165, 47p
- York D. G. et al., 2000, *AJ*, 120, 1579

This paper has been typeset from a $\text{\TeX}/\text{\LaTeX}$ file prepared by the author.